

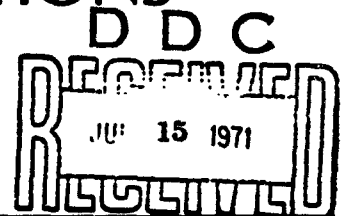
AD 729757

R-666-PR

May 1971

# THE EQUATION OF STATE OF WATER AT HIGH TEMPERATURES AND PRESSURES, A PRELIMINARY TO DAMAGE CALCULATIONS

R. A. Papetti and M. C. Fujisaki



A Report prepared for  
UNITED STATES AIR FORCE PROJECT RAND

Reproduced by  
NATIONAL TECHNICAL  
INFORMATION SERVICE  
Springfield, Va. 22151

**Rand**  
SANTA MONICA, CA 90406

DISTRIBUTION STATEMENT A  
Approved for public release;  
Distribution Unlimited

# DOCUMENT CONTROL DATA

1. ORIGINATING ACTIVITY  The Rand Corporation		2a. REPORT SECURITY CLASSIFICATION UNC LASSIFIED	
		2b. GROUP	
2. REPORT TITLE  THE EQUATION OF STATE OF WATER AT HIGH TEMPERATURES AND PRESSURES, A PRELIMINARY TO DAMAGE CALCULATIONS			
4. AUTHOR(S) (Last name, first name, initial) Papetti, R. A., M. C. Fujisaki			
3. REPORT DATE May 1971	6a. TOTAL NO. OF PAGES 76	6b. NO. OF REFS. 25	
7. CONTRACT OR GRANT NO. F44620-67-C-0045	8. ORIGINATOR'S REPORT NO. R-666-PR		
9a. AVAILABILITY/LIMITATION NOTICES DDC-1		9b. SPONSORING AGENCY United States Air Force Project Ra	
10. ABSTRACT  Third and last of a series documenting the thermodynamic relations of water at high temperatures and pressures, such as might be caused by a nuclear burst. This report evaluates the Becker-Kistiakowsky-Wilson equation--also known as the Halford-Kistiakowsky-Wilson or HKW equation; tests modifications proposed by various Los Alamos researchers; and proposes some new modifications. In the thermochemical region, calculations are primarily a matter of interpolation between areas of known results and accepted physical theory to obtain equations of state for the large missing area. The authors therefore redesign the state equations so as to achieve a smooth joining of the Thomas-Fermi model results at 20 megabars with experimental data on the Hugoniot curve under 1 megabar. This required treating some BKW constants as functions of thermodynamic coordinates, and calculating pressure/specific volume/internal energy relations for the region above about 300 kilobars.		11. KEY WORDS  Thermodynamics Physics Chemistry Nuclear physics	

6-17-71

**CORRIGENDUM**

**R-666-PR**    **THE EQUATION OF STATE OF WATER AT HIGH TEMPERATURES AND PRESSURES: A PRELIMINARY TO DAMAGE CALCULATIONS, by R. A. Papetti, M. C. Fujisaki, May 1971 Unclassified**

**COMMUNICATION  
DEPARTMENT**

**p. 45, Figure 18: The scale on the ordinate should read (reading up) '10<sup>2</sup>', '10<sup>3</sup>', '10<sup>4</sup>'.**

**Rand**  
SANTA MONICA, CA 90406

R-666-PR

May 1971

# THE EQUATION OF STATE OF WATER AT HIGH TEMPERATURES AND PRESSURES, A PRELIMINARY TO DAMAGE CALCULATIONS

R. A. Papetti and M. C. Fujisaki

A Report prepared for  
UNITED STATES AIR FORCE PROJECT RAND

**Rand**  
SANTA MONICA, CA 90406

*Rand maintains a number of special subject bibliographies containing abstracts of Rand publications in fields of wide current interest. The following bibliographies are available upon request:*

*Africa • Arms Control • Civil Defense • Combinatorics  
Communication Satellites • Communication Systems • Communist China  
Computing Technology • Decisionmaking • Delphi • East-West Trade  
Education • Foreign Aid • Foreign Policy Issues • Game Theory  
Health-related Research • Latin America • Linguistics • Maintenance  
Mathematical Modeling of Physiological Processes • Middle East  
Policy Sciences • Pollution • Program Budgeting  
SIMSCRIPT and Its Applications • Southeast Asia • Systems Analysis  
Television • Transportation • Urban Problems • USSR/East Europe  
Water Resources • Weapon Systems Acquisition  
Weather Forecasting and Control*

*To obtain copies of these bibliographies, and to receive information on how to obtain copies of individual publications, write to: Communications Department, Rand, 1700 Main Street, Santa Monica, California 90406.*

PREFACE

This Report represents the culmination of an effort begun several years ago. The United States Air Force was examining the feasibility of alternative systems of missile basing, and became interested in accurately calculating the pressures and motions following a nuclear burst in or near water. Such calculations are necessary to establish estimates of damage to nearby structures.

The material in the Report is highly technical, and is basic to an understanding of the physical behavior of water at high temperatures and pressures. The results presented should have lasting utility, not only for their original purpose of damage assessment, but in a wide variety of applications.

This Report is the third and last in a series that documents results on the determination of thermodynamic relations for water; the others are RM-4969 and RM-5050.

### SUMMARY

The BKW equation is an empirical relation for the pressure-volume-temperature equation of state of a nonideal mixture of gases. This equation and some of its numerous modifications have been used as a basis for determining thermodynamic relationships for gaseous mixtures at high pressures and densities. In this Report, we test the BKW equation and some of its recent modifications for use in determining a set of thermodynamic relations for water over a wide range of pressures, temperatures, and densities. On the basis of the results of these tests, we propose a further group of modifications that would provide improved thermodynamic relations for use in calculations simulating nuclear bursts in or near water.

We test our various proposed modifications, and recommend one of them on the basis of our results. Finally, we calculate a pressure-specific volume-internal energy relation, based on our modified form of the BKW equation, that can be used above approximately 300 kilobars.

The detailed results of the study are summarized on pp. 50-52 of this Report.

CONTENTS

PREFACE. . . . .	111
SUMMARY. . . . .	v
SYMBOLS. . . . .	ix
Section	
I. INTRODUCTION. . . . .	1
II. THE BECKER-KISTIAKOWSKY-WILSON EQUATION . . . . .	9
III. VARIABLE BKW PARAMETERS . . . . .	12
IV. SUMMARY OF WORKING EQUATIONS. . . . .	15
V. HUGONIOT COMPUTATIONS, REGION I . . . . .	17
All Parameters Treated as Constants : . . . . .	17
Constant $\kappa$ , Variable $\beta$ . . . . .	21
$\kappa$ As a Function of Temperature. . . . .	22
$\kappa$ As a Function of $\bar{x}$ . . . . .	25
VI. RESULTS ON ISOTHERMS AND ISOMETRICS, REGION I . . . . .	32
VII. HUGONIOT CALCULATIONS, REGION II. . . . .	43
VIII. RESULTS ON ISOTHERMS AND ISOMETRICS, REGION II. . . . .	47
IX. SUMMARY OF RESULTS AND DISCUSSION . . . . .	50
Appendixes	
A. SUMMARY OF THERMODYNAMIC RELATIONS BASED ON THE THERMAL (p,V,T) EQUILIBRIUM EQUATIONS . . . . .	53
B. SUMMARY OF THERMODYNAMIC RELATIONS BASED ON THE MODIFIED BKW EQUATION WITH $\beta = \beta(T)$ , $\kappa = \kappa(T)$ . . . . .	56
C. SUMMARY OF THERMODYNAMIC RELATIONS BASED ON THE MODIFIED BKW EQUATION WITH $\beta = \beta(T)$ , $\kappa = \kappa(\bar{x})$ . . . . .	59
D. BRIEF OUTLINE OF THE COMPUTATIONAL METHOD FOR EQUILIBRIUM CALCULATIONS IN REGIONS I AND II. . . . .	62
REFERENCES . . . . .	65

SYMBOLS

- A = Helmholtz free energy of mixture
- c = number of species in mixture
- E = internal energy of mixture
- F = Gibbs free energy of mixture
- H = enthalpy of mixture
- h = specific enthalpy
- $M_o$  = mass of one gram-mol of water
- $n_g$  = total mols of mixture
- $n_i$  = mols of the  $i^{\text{th}}$  component in mixture
- p = pressure
- $p^o$  = standard state pressure (1 atm)
- $p_o$  = pressure at center point of the Hugoniot (1 atm)
- $\tilde{R}$  = molar gas constant
- r = distance between centers of two molecules
- S = entropy of mixture
- T = temperature
- $T_o$  = 298.16°K
- V = total volume =  $M_o v$
- $V^o$  = total volume of mixture at pressure  $p^o$ ,  $V^o = n_g \tilde{R}T/p^o$
- v = specific volume
- $x_i$  = mol fraction of  $i^{\text{th}}$  species
- $y_1$  = mols of atomic hydrogen
- $y_2$  = mols of atomic oxygen
- $y_3$  = mols of electrons

-x-

- $\mu_j$  = chemical potential of  $j^{\text{th}}$  species in mixture
- $\nu_{ij}$  = stoichiometric coefficient of  $j^{\text{th}}$  species in  $i^{\text{th}}$  reaction
- $\phi$  = intermolecular potential

#### Superscripts

- ' = differentiation; e.g.,  $\kappa'(T) = d\kappa/dT$
- ~ = molar quantity
- o = material at temperature T in its standard state (ideal gas at 1 atm)
- \* = a residual (imperfection) contribution to a thermodynamic quantity (except for  $T^*$ )

#### Subscripts

- o = ambient conditions = liquid water at 298.16° and 1 atm
- i, j, k = index representing  $(i,j,k)^{\text{th}}$  reaction, or  $(i,j,k)^{\text{th}}$  species

## I. INTRODUCTION

The material presented here represents results from a portion of the studies that have been directed toward the development of equations of state of water suitable for high-energy and hydrodynamic computations. In this report, we review current forms of the BKW equation of state (discussed in the following section) and recommend some modifications of its currently accepted form. We also test both the existing BKW equation and our modified versions for their suitability in hydrodynamic computations over a wide range of pressures and temperatures. Although these results were obtained some time ago, they are still relevant to the major unsolved problem of obtaining the equations of state needed to theoretically predict the motions and stresses following a nuclear burst in water. Results based on the studies presented here cover a significant portion of the entire pressure and temperature range needed in such computations. A recommended set of equations covering the entire range of interest and containing the results of this study will be published in the near future.

The following investigation is based on the thermochemical program developed in Ref. 1. Using the general outline of that reference, we divided the pressure-volume plane into a series of distinct regions, shown in Fig. 1. In the highest-pressure region, we used the equation-of-state results of A. Latter and R. Latter based on the Thomas-Fermi method. Below the Thomas-Fermi region, the  $H_2O$  molecule has decomposed into the twenty-three species of Table 1, which are assumed to be in chemical equilibrium for temperatures above  $5000^\circ K$  (Region I of Fig. 1). Calculations using the BKW equation of state have shown that more than 99 mol percent of the mixture consists of six species ( $H$ ,  $O$ ,  $H_2$ ,  $O_2$ ,  $H_2O$ , and  $OH$ ) at temperatures of  $5000^\circ K$  and  $7000^\circ K$ . Therefore, in Region II of Fig. 1, only these six species are assumed to exist. Below  $2000^\circ K$  (Region III), BKW calculations show that the  $H_2O$  molecules remain essentially intact. Thus the  $2000^\circ K$  isotherm is established as the lower boundary of Region II. Regions I and II cover the greatest portion of the pressure-volume plane over which the BKW equation of state will be modified and tested to determine thermodynamic relations

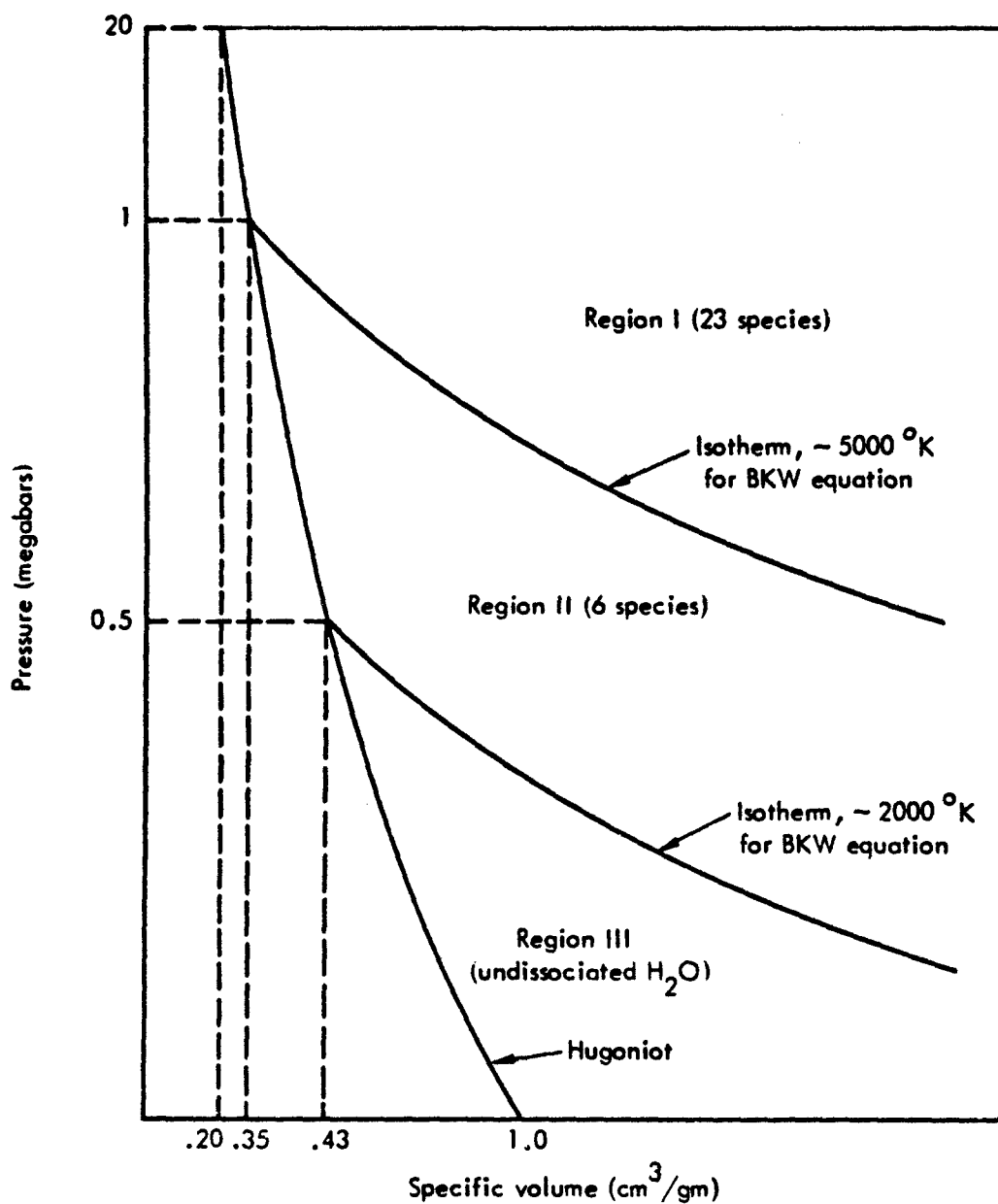


Fig. 1—Approximate regions of the BKW equilibrium studies. All values shown of the sketch are approximate. Isotherms and Hugoniot shown are illustrative only.

Table 1

SPECIES AND REACTIONS FOR THE CHEMICAL EQUILIBRIUM PROBLEM IN WATER

Species Number	Species	Reaction Number	Reaction
1	$O^+$	1	$O = O^+ + e$
2	$O^{+2}$	2	$O = O^{+2} + 2e$
3	$O^{+3}$	3	$O = O^{+3} + 3e$
4	$O^{+4}$	4	$O = O^{+4} + 4e$
5	$O^{+5}$	5	$O = O^{+5} + 5e$
6	$O^{+6}$	6	$O = O^{+6} + 6e$
7	$O^{+7}$	7	$O = O^{+7} + 7e$
8	$O^{+8}$	8	$O = O^{+8} + 8e$
9	$H^+$	9	$H = H^+ + e$
10	$O_2$	10	$2O = O_2$
11	$O_2^+$	11	$2O = O_2^+ + e$
12	$H_2$	12	$2H = H_2$
13	$H_2^+$	13	$2H = H_2^+ + e$
14	$H_2O$	14	$2H + O = H_2O$
15	$OH$	15	$O + H = OH$
16	$OH^-$	16	$O + H + e = OH^-$
17	$OH^+$	17	$O + H = OH^+ + e$
18	$O^-$	18	$O + e = O^-$
19	$H^-$	19	$H + e = H^-$
20	$O_2^{+2}$	20	$2O = O_2^{+2} + 2e$
21	$H$		
22	$O$		
23	$e$		

Source: Ref. 1.

for water. The various species which may occur in Region I are shown in Table 1. Stoichiometric coefficients for reactions among the species of Table 1 are shown in Tables 2 and 3. The upper limit on Region I is roughly established at 20 megabars, corresponding to our estimate of the lower limit of validity of the Thomas-Fermi calculations of A. Latter and R. Latter<sup>(2)</sup> for  $H_2O$  at extreme pressures.

The reasons for terminating the low-pressure results of Latter and Latter are indicated in Fig. 2, which contains the Hugoniot results of Ref. 2 at the high pressures and experimental Hugoniot points at the lower pressures.<sup>(3,4)</sup> At pressures below roughly 20 megabars, the Thomas-Fermi model shows a tendency to predict pressures which are too high. This deviation of the Hugoniot is consistent with the oft-repeated statement that the Thomas-Fermi model should not be used below a pressure of approximately 10 megabars.<sup>(5,6)</sup> Since this comment applies to the heavier elements, which more generally satisfy the assumption of a Thomas-Fermi analysis than the  $H_2O$  molecule, the apparent deviations of Fig. 2 are not surprising. (At a temperature of 298°K and a volume of 1 cm<sup>3</sup>/gm, which correspond to normal liquid-water conditions, the Thomas-Fermi model predicts a pressure of approximately 350 kilobars.) Rice and Walsh<sup>(4)</sup> have developed an equation of state of water to 250 kilobars which is applicable to a region near the Hugoniot, and Walker and Sternberg<sup>(7)</sup> have constructed a pressure-volume-energy equation for water in the region bounded on the left in a p-v diagram by the Hugoniot and on the right by the adiabat which intersects the Hugoniot at 250 kilobars. A p-v-T relation to 1 megabar and 10,000°C has been developed by Howard.<sup>(8)</sup> These investigations cover only a small portion of the region over which we are seeking equilibrium solutions. To our knowledge, the investigations of Snay and coworkers<sup>†</sup> represent the most systematic attempt to obtain equilibrium relations for water in the regions of Fig. 1.

The principal analytical tool used in their investigations, the Becker-Kistiakowsky-Wilson (BKW)<sup>††</sup> equation, has since been modified

<sup>†</sup>See Refs. 9, 10, 11, and 12.

<sup>††</sup>This same relation is often referred to as the Halford-Kistiakowsky-Wilson (HKW) equation.

Table 2  
STOICHIOMETRIC COEFFICIENTS ( $v_{ij}$ ) FOR THE REACTIONS OF REGION I

Species Number	Reaction Number																			
	1	2	3	4	5	6	7	8	9	10	11	12	13	14	15	16	17	18	19	20
1	1																			
2		1																		
3			1																	
4				1																
5					1															
6						1														
7							1													
8								1												
9									1											
10										1										
11											1									
12												1								
13													1							
14														1						
15															1					
16																1				
17																	1			
18																		1		
19																			1	
20																				1
21									-1			-2	-2	-2	-1	-1	-1		-1	
22	-1	-1	-1	-1	-1	-1	-1	-1		-2	-2			-1	-1	-1	-1	-1		-2
23	1	2	3	4	5	6	7	8	1		1		1			-1	1	-1	-1	2

Note: A blank space in the table signifies a zero value for the stoichiometric coefficient.

Table 3

PARTIAL DATA SUMMARY FOR THE EQUILIBRIUM-WATER-THERMOCHEMICAL PROBLEM

Reaction Number	Species	$r_{11}$	$r_{21}$	$r_{31}$	$\sum_{j=1}^c v_{1j}$
1	$O^+$	0	1	1	1
2	$O^{+2}$	0	1	2	2
3	$O^{+3}$	0	1	3	3
4	$O^{+4}$	0	1	4	4
5	$O^{+5}$	0	1	5	5
6	$O^{+6}$	0	1	6	6
7	$O^{+7}$	0	1	7	7
8	$O^{+8}$	0	1	8	8
9	$H^+$	1	0	1	1
10	$O_2$	0	2	0	-1
11	$O_2^+$	0	2	1	0
12	$H_2$	2	0	0	-1
13	$H_2^+$	2	0	1	0
14	$H_2O$	2	1	0	-2
15	$OH$	1	1	0	-1
16	$OH^-$	1	1	-1	-2
17	$OH^+$	1	1	1	0
18	$O^-$	0	1	-1	-1
19	$H^-$	1	0	-1	-1
20	$O_2^{+2}$	0	2	2	1

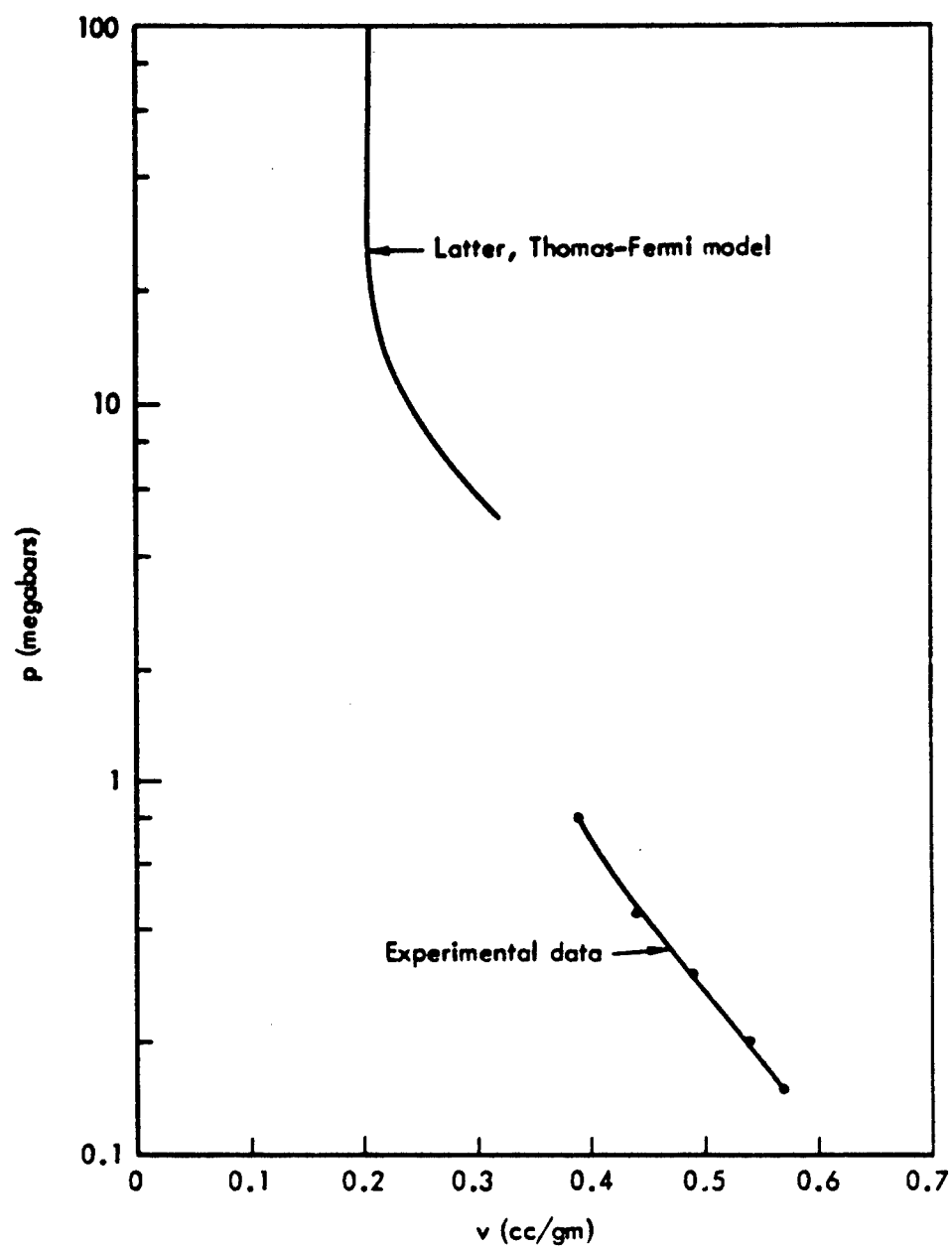


Fig.2—Experimental and Thomas-Fermi Hugoniot curves for water

and improved by various investigators at Los Alamos. (13,14,15) We attempt here to capitalize on these improvements to obtain perhaps more accurate thermodynamic relations than those reported for water in Refs. 11 and 12.<sup>†</sup> We also attempt to estimate the range of validity of results obtained by our version of the BKW equation.

---

<sup>†</sup> In Ref 12, the BKW modifications of Ref. 15 are recommended. As a starting point, we will use the most recent BKW parameters of Ref. 14, which show better agreement with experimental Hugoniot data than those of Ref. 15.

## II. THE BECKER-KISTIAKOWSKY-WILSON EQUATION

For  $M_0$  grams ( $n_g$  mols) of a pure substance, the BKW equation, with its most recent modifications, takes the form

$$\frac{pV}{n_g \tilde{RT}} = 1 + x e^{\beta x}, \quad (1)$$

$$x = \frac{\kappa k}{V(T + \theta)^\alpha}, \quad (2)$$

where the parameters  $\beta$ ,  $\kappa$ ,  $\alpha$ ,  $\theta$ , and  $k$  are constants.<sup>†</sup> The total volume,  $V$ , may also be expressed as  $V = M_0 v$  whenever we wish to present results in terms of specific volume,  $v$ .

The variable  $x$  in Eq. (2) bears a resemblance to a familiar ratio in the theory of imperfect gases:

$$x \sim \frac{\text{Covolume}^{\dagger\dagger} \text{ of } M_0 \text{ mass of material}}{\text{Total volume of } M_0 \text{ mass of material}}.$$

If the parameter  $\theta$  were not present (and it wasn't in the original form of the equation), the temperature-dependence of  $x$  would be that achieved by molecules with a repulsive pair potential of exponent  $3/\alpha$ :

$\phi(r) = r^{-3/\alpha}$ , where  $r$  is the internuclear distance between two interacting molecules.

For a mixture of  $c$  species of composition  $\underline{n} = \{n_1, \dots, n_c\}$  ( $n_j$ , where  $j = 1 \dots c$ , represents the number of mols of the  $j^{\text{th}}$  species in a mixture of mass  $M_0$ ), the covolume factor,  $k$  of Eq. (2) is replaced by an average covolume factor

<sup>†</sup>The resolution of the constant in the numerator of Eq. (2) into a product will become clearer when we discuss the form of the equation for mixtures.

<sup>††</sup>The covolume of a gas is equal to 4 times the volume of molecules treated as rigid spheres, and roughly represents the volume unavailable to the centers of the molecules. The covolume factor (p. 10 and following text) is an empirical constant that resembles the covolume.

$$k = \sum_{i=1}^c n_i k_i ,$$

where  $k_i$  is the covolume factor of the  $i^{\text{th}}$  species.

Equations (1) and (3) form the starting point of our equilibrium calculations:

$$x = \frac{\kappa \sum_{i=1}^c n_i k_i}{V(T + \theta)^\alpha} . \quad (3)$$

The parameters  $\kappa$ ,  $\theta$ ,  $\alpha$ ,  $\theta$ , and all of the covolume factors,  $k_i$ , are regarded as empirical material constants to be determined by experiments. These are usually detonation experiments, performed with a variety of explosives with different product compositions, where the above parameters are chosen to best predict experimental curves of detonation velocity versus loading density, and Chapman-Jouguet temperatures and pressures.<sup>†</sup>

The strongly empirical nature of the BKW equation has been the principal source of a number of warnings<sup>(14,15)</sup> issued against its use in an extended extrapolation of experimental results either to high pressures and densities or to materials (such as, for example,  $O^{+5}$  in Table 1) that did not appear in the experiments used to choose the parameters of the problem. However, the studies of Refs. 18, 19, 20, and 21 provide little motivation to use more complicated equations of state, more sophisticated intermolecular potentials, or more physically plausible mixture theories for calculations in our high-density, high-pressure region, since such methods have not led to results that were clearly superior to those obtained via the BKW equation at experimentally attainable pressures and densities. Molecular theories for equi-

---

<sup>†</sup> For further information on this subject, we refer the reader to Refs. 13, 14, 15, and 16. Chapman-Jouguet theory is discussed in Ref. 17. The use of detonation theory and detonation experiments to set empirical constants in equations of state based on intermolecular potentials are discussed in Refs. 18, 19, 20, and 21.

librium calculations in mixtures below the Thomas-Fermi region are based on the use of spherical, additive pair potentials to represent the forces acting on a molecule. Such calculations are all semiempirical, for the pair potentials on which they are based contain force constants, which must be established by experiment for most materials. In addition, the assumption of spherical, additive pair potentials becomes unreliable at pressures as high as those contemplated in our calculations, even for such normally well-behaved materials as the noble gases,<sup>(21,22,23)</sup> and we are by no means dealing with well-behaved materials. Thus, the physical theories based on molecular models contain many of the undesirable traits that plague the BKW equation. It appears that the region between experimental data and the Thomas-Fermi model cannot be treated in an entirely satisfactory manner, and that each of the current methods of analysis assumes more the aspect of an interpolation than a physical theory when applied to this region. At the same time however, extrapolations of the BKW equation to infinite pressures, such as appear in Refs. 11 and 12, place considerably greater faith in the validity of this equation than it deserves. The approach taken here represents a compromise between the two conflicting views and usages of the BKW equation at extreme pressures.

We tentatively accept the BKW equation as an interpolation formula between 1 and 20 megabars. Its parameters are then adjusted so that its pressure-volume Hugoniot curve joins the Thomas-Fermi Hugoniot at about 20 megabars, and the experimental data at about one megabar. We next test the resulting form of the BKW equation on isotherms and isometrics to see how well our modifications reproduce known results at high and low pressures. We then recommend use of the unmodified or modified forms of the BKW relations only for those thermodynamic variables that show reasonable agreement with known results, and only over the estimated ranges where agreement does occur. As we will show later, the Hugoniot-matching conditions require treating certain BKW parameters, hitherto held constant, as functions of one or more thermodynamic coordinates.

### III. VARIABLE BKW PARAMETERS

To decide which of the parameters  $\kappa$ ,  $\beta$ ,  $\alpha$ ,  $\theta$ , and  $k_1$  should assume the role of variables rather than constants, and what their functional forms should be, we use the following three guidelines: (1) We will seek simple working equations. (2) We wish to vary as few parameters as possible and still achieve our previously stated objective of forcing BKW results into high- and low-pressure results of other solutions or data. The more terms we vary, the more we defeat our first goal of maintaining simple forms for computation. (3) We prefer to vary those parameters which lend themselves to some physical interpretation. In this way we can more confidently predict the general consequences of an assumed variation. A physical interpretation of the parameter usually places reasonable bounds on the range of values which may be assumed by that parameter. For instance, we know that the covolume factors should always remain positive. Therefore, a range of  $\kappa$  which includes negative values would be unreasonable. It would, on the other hand, be difficult physically to justify the prohibition of negative values for the range of the parameters  $\beta$  and  $\theta$  for temperatures larger than  $\theta$ .

The individual terms  $\kappa k_1$  are proportional to the molecular volume of the  $i^{\text{th}}$  component of the mixture. Each of these individual terms could be varied, but there are twenty-three in all, and assuming an independent variation of each would create computational difficulties well beyond those that we would care to encounter. Besides, there is little information available to us to decide how each species should change relative to all of the others. The common factor,  $\kappa$ , on the other hand, can be varied without introducing too many subsequent difficulties into our computer programs, and can still be thought of as yielding a physical effect. We can consider the molecules of the mixture as becoming "softer" and "harder," respectively, with decreasing and increasing  $\kappa$ . The variation of  $\kappa$ , rather than the individual molecular constants  $k_1$ , implies that the molecular volume of each species grows or decreases proportionately, which, though not entirely accurate, represents at least a plausible manner for molecules of a mixture to change their size. The parameter  $\beta$  has little physical significance,

except what can be gleaned from Eq. (1) and a knowledge of the fact that  $x \geq 0$ . We see from this equation that an increase in  $\delta$  represents an increase in the compressibility factor,  $p\tilde{V}/RT$ , and thus a greater departure from ideality (i.e., the ideal gas relation,  $p\tilde{V} = RT$ ). Treating  $\delta$  as a variable would not severely complicate the forms of the equations, for it does not appear in the definition of  $x$ . The parameter  $\alpha$  appears in the BKW equation in a considerably more complicated way than  $\delta$  or  $\kappa$ . We therefore do not care to vary  $\alpha$  if we can avoid it. Finally, the parameter  $\theta$  cannot be assigned any kind of physical interpretation that we can think of, and in addition would have to vary strongly at the higher temperatures to have any significant effect on the solutions. We therefore hold  $\theta$  constant at its current value of 400°K. On the basis of these remarks, we have elected to vary the parameters  $\kappa$  and  $\delta$  and to treat  $k_1$ ,  $\alpha$ , and  $\theta$  as constants.

There still remains the problem of choosing the independent variables for the functions defining  $\kappa$  and  $\delta$ . The independent variables of the entire equilibrium problem are temperature and volume. These would appear to be the best choice of independent variables for  $\kappa$  and  $\delta$ . The residual internal energy and residual Helmholtz free energy are obtained by integrating the expressions  $T(\partial p/\partial T)_V - p$  and  $p$ , respectively, with volume ( $v$ ) at constant temperature ( $T$ ) and composition  $n$ .<sup>†</sup> This integration is most efficiently carried out for the BKW equation by replacing  $V$  by  $x$  as an independent variable via the differential relation

$$\frac{dV}{V} = - \frac{dx}{x} \quad T, n = \text{constant}$$

The forms of the functions would therefore be subject of simplification if  $\kappa$  and  $\delta$  were functions of  $x$  rather than  $V$ . In addition, the value of  $x$  is a better index of the departure of the material from ideality than  $V$ . Indeed, if  $\delta$  were not a function of  $T$  (and it will not be in our final results),  $x$  would be uniquely related to the

<sup>†</sup>See Ref. 1 for a discussion of these integrations.

compressibility factor,  $p\tilde{V}/RT$ . Therefore  $T$  and  $x$  appear suitable choices for the independent variables.

Although we have narrowed the choice down to the two functions

$$\kappa = \kappa(x, T), \quad \beta = \beta(x, T),$$

these are still too general for the numerical study needed to establish their approximate forms. Once again, in the name of convenience, we limit ourselves to two simple possibilities:

$$\beta = \beta(T); \quad \beta = \kappa(T) \quad (4a)$$

$$\beta = \beta(T); \quad \kappa = \kappa(x). \quad (4b)$$

The equilibrium relations for the pressure, internal energy, Helmholtz free energy, chemical potentials, and equilibrium constants as functions of temperature and specific volume will be presented in the next section for relations (4a) and (4b).

#### IV. SUMMARY OF WORKING EQUATIONS

The thermodynamic equations developed in this section pertain to a mixture composed of the twenty-three species appearing in Table 1, which are in chemical, thermal, and mechanical equilibrium, and whose parameters fall into one of the two following categories:

A:  $\alpha, \theta, k_1 = \text{constant}$

$$\beta = \beta(T), \quad \kappa = \kappa(T);$$

B:  $\alpha, \theta, k_1 = \text{constant}$

$$\beta = \beta(T), \quad \kappa = \kappa(x).$$

Because the equations for Region II and the equations corresponding to constants  $\beta$  and  $\kappa$  are all special cases of the relations which we will obtain, there is no need to discuss these cases separately.

The equations in terms of an arbitrary p-v-T relation are developed in Ref. 1. A summary of those results is given in Appendix A.

The working equations of category A are obtained by substituting Eqs. (1) and (3) for pressure into the equations of Appendix A, using

$$\alpha, \theta, k_1 = \text{constant}, \quad \beta = \beta(T), \quad \kappa = \kappa(T)$$

wherever these quantities occur in Eqs. (1) and (3).

Reduction of the equations to forms suitable for computation follows a pattern very close to that of the test problem in Ref. 1. Those who are interested in pursuing the details should use the test problem as a guide. We limit ourselves here to a presentation of the final results, which appear in Appendix B.

The equations of category B follow a pattern of development entirely similar to those of category A. For convenience, we have taken  $\kappa$  to be a function of  $\bar{x}$ , which is defined by

$$\bar{x} = \frac{\sum_{i=1}^{23} n_i k_i}{V(T + \theta)^\alpha} . \quad (5)$$

Requirements for the equivalence of  $x$  and  $\bar{x}$  as choices of independent variable for  $\kappa$  follow from their relation to one another,

$$\kappa \bar{x} = x . \quad (6)$$

The values of the variables  $\kappa$ ,  $x$ , and  $\bar{x}$  are all greater than zero. Therefore, for each continuous functional dependence  $H(x)$  assigned to  $\kappa$ , there is a reciprocal one-to-one correspondence between  $x$  and  $\bar{x}$  via the relation  $x/H(x) = \bar{x}$ , provided the function  $x/H(x)$  is monotone for positive values of  $x$  and  $H(x)$ . The functions we will use,

$$\kappa(\bar{x}) = K \bar{x}^\gamma, \quad K, \gamma = \text{constants} > 0,$$

satisfy these requirements on  $\kappa(x)$ .

The equations which are used for computations based on parameters in category B appear in Appendix C.

# V. HUGONIOT COMPUTATIONS, REGION I

## ALL PARAMETERS TREATED AS CONSTANTS

Our parametric studies are performed on the p-v shock Hugoniot centered at  $p_0 = 10^{-6}$  megabars,  $v_0 = 1 \text{ cm}^3/\text{gm}$  ( $V_0 = M_0 v_0 \text{ cm}^3$ ), which corresponds to ambient fresh water. There is no loss in the accuracy of our results if we set  $p_0$  equal to zero. The Hugoniot relation becomes

$$E(T, V, \eta) = \frac{1}{2} p(T, V, \eta) (V_0 - V) . \quad (7)$$

The internal energy function  $E(T, V, \eta)$  has been defined so that  $E_0 = 0$ . This explains the absence of  $E_0$  in Eq. (7).

Our first Hugoniot parameter study covers Region I, and is based entirely on constant parameters. For this particular case the equations of Appendix B and those of Appendix C are equivalent. The equations of Appendix B are most easily reduced to the present case. The computer runs made with constant values of the parameters are used to decide which of the four sets of covolume factors,  $k_1$ , appearing in Table 4 should be used.

We use Mader's<sup>(14)</sup> recommended values for  $\kappa$ ,  $\beta$ ,  $\alpha$ , and  $\theta$  based on detonation calculations using RDX as the explosive. They have the values shown in set 1, Table 5.

We chose the parameters in Ref. 14 based on the explosive RDX rather than TNT because our system contains no carbon (see Ref. 14).<sup>†</sup> The method of computations used is discussed briefly in Appendix D. Computations have been carried out in Region I for all four sets of covolume factors to determine which set comes closest to reproducing the Thomas-Fermi Hugoniot at high pressures. The results are shown in Fig. 3, along with the Hugoniot results of Ref. 12, using an older

<sup>†</sup>The four sets of covolume factors in Table 4 are those of Ref. 12, with covolume factors for  $H_2$ ,  $O_2$ , and  $H_2O$  changed to the values recommended in Ref. 14.

Table 4

COVOLUME FACTORS AND WEIGHTED SUMS OF COVOLUME FACTORS  
USED IN BKW PARAMETER STUDIES; REGION I\*

Species Number	Set 1		Set 2		Set 3		Set 4	
	$k_1$	$\sum_{j=1}^c v_{j1} k_j$	$k_1$	$\sum_{j=1}^c v_{j1} k_j$	$k_1$	$\sum_{j=1}^c v_{j1} k_j$	$k_1$	$\sum_{j=1}^c v_{j1} k_j$
1	80	- 20	80	- 20	120	- 30	120	- 30
2	65	- 35	65	- 35	98	- 52	98	- 52
3	54	- 46	54	- 46	80	- 70	80	- 70
4	45	- 55	45	- 55	67	- 83	67	- 83
5	38	- 62	38	- 62	57	- 93	57	- 93
6	0.3	-100	0.3	-100	0.5	-150	0.5	-150
7	0.3	-100	0.3	-100	0.4	-150	0.4	-150
8	0	-100	0	-100	0	-150	0	-150
9	0	- 20	0	- 40	0	- 30	0	- 60
10	350	150	350	150	350	50	350	50
11	255	55	255	55	255	- 45	255	- 45
12	180	140	180	100	180	120	180	60
13	50	10	100	20	50	- 10	100	- 20
14	250	110	250	70	250	40	250	- 20
15	200	80	200	60	200	20	200	- 10
16	230	110	230	90	230	50	230	20
17	170	50	170	30	170	- 10	170	- 40
18	115	15	115	15	173	23	173	23
19	25	5	50	10	38	8	75	15
20	240	40	240	40	240	- 60	240	- 60
21	20		40		30		60	
22	100		100		150		150	
23	0		0		0		0	

\* All covolumes except those for species 10, 12, and 14 ( $H_2O$ ,  $O_2$ ,  $H_2O$  respectively) are from Ref. 12. Covolumes for species 10, 12, and 14 are from Ref. 14.

Table 5  
THREE SETS OF PARAMETERS USED IN BKW CALCULATIONS, REGION I

Set Number	$\alpha$	$\beta$	$\theta(^{\circ}\text{K})$	$k_1 \frac{\text{cm}^3 \text{K}^{\frac{1}{2}}}{\text{mol}}$	$\kappa$
(1) $\kappa = \text{const}$	0.50	0.16	400	Set 1 Table 4	10.91
(2) $\kappa = \kappa(T)$	0.50	0.16	400	Set 1 Table 4	$\frac{10.91}{1 + \frac{T - 5000}{75000}}$
(3) $\kappa = \kappa(\bar{x})$	0.50	0.16	400	Set 1 Table 4	$10.91 \left( \frac{\bar{x}}{.50566} \right)^{0.8}$

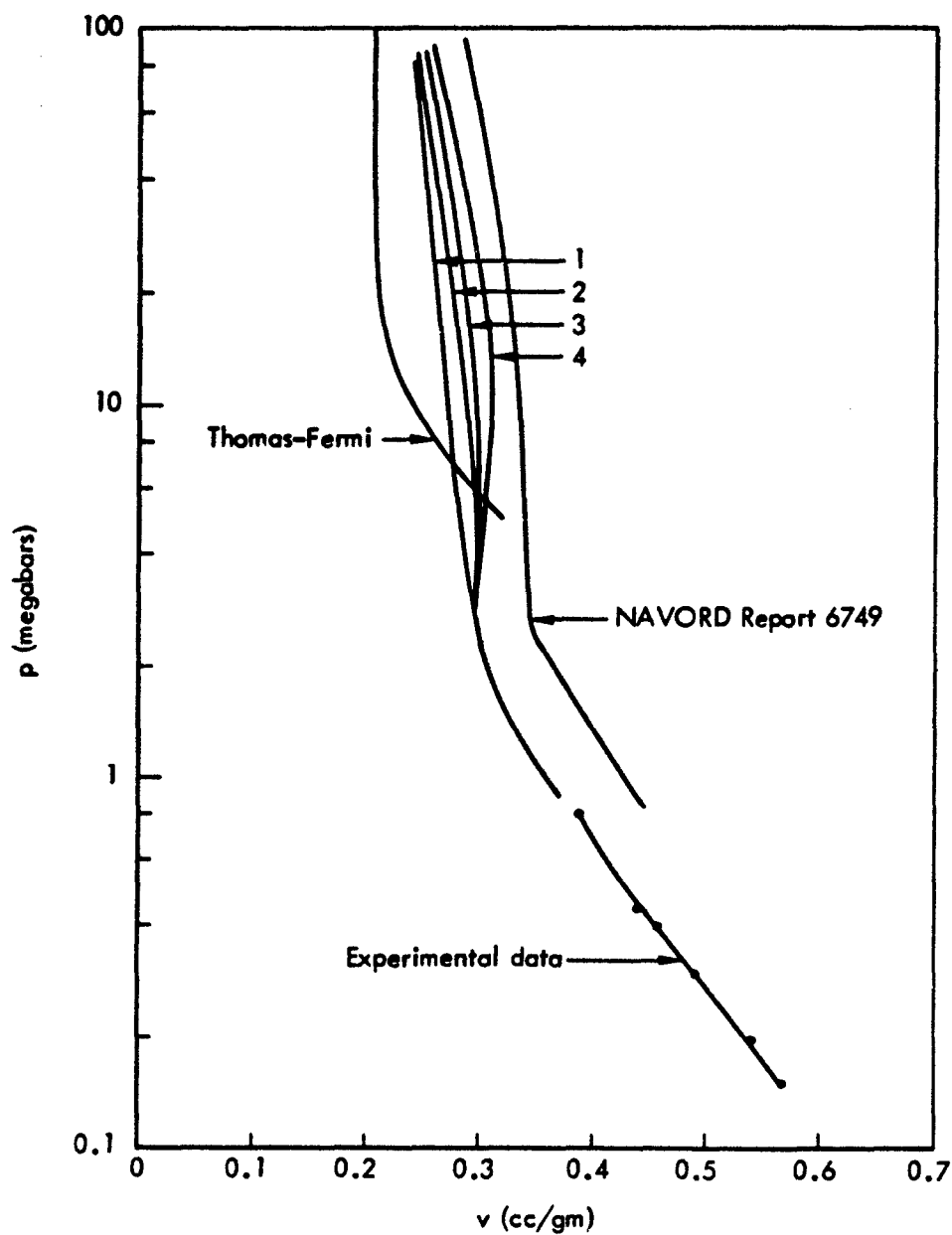


Fig.3—BKW Hugoniot curves, Region I. The four numbered curves correspond to the first set of parameters (Table 6) and the four sets of covolume factors (Table 4)

set of BKW parameters. From Fig. 3 we see that all four solutions based on the parameters of Ref. 14 and the (modified) covolume factors of Ref. 12 represent a considerable improvement at the lower pressures over the solutions appearing in Ref. 12. However, none of the four p-v Hugoniot solutions obtained match the Thomas-Fermi Hugoniot solutions at the higher pressures. The leftmost Hugoniot curve (curve 1), based on the first column of covolume factors appearing in Table 4, is closest to the Thomas-Fermi Hugoniot. We therefore chose this set of covolume factors for our subsequent programs.

#### CONSTANT $\kappa$ , VARIABLE $\beta$

It is clear from Fig. 3 that our BKW Hugoniot, curve (1), is too steep at the high pressures. That is, for the portion of the curve in the Thomas-Fermi region, the Hugoniot pressures corresponding to a given specific volume are much higher than those predicted by the Thomas-Fermi model. The material based on the BKW equation with constant parameters appears, therefore, to be too hard. Our first attempts to soften the material were based on variations of  $\beta$  with temperature. If we attribute the steepness of the Hugoniot curve to excessive departure of the BKW equation from ideality, then it is evident from Eqs. (1) and (2) and the condition  $x \geq 0$  that we want  $\beta$  to decrease as the Hugoniot pressures increase. Since temperatures increase on the Hugoniot with increasing pressures, we must construct functions  $\beta(T)$  that have the appropriate value of 0.16 at a temperature of 5000°K, and that decrease monotonically with temperature for temperatures greater than 5000°K.

Two functional forms meeting these conditions, which we used in Hugoniot calculations, are

$$\hat{\beta}(T) = \hat{\beta}_2 + \frac{\hat{\beta}_2 - 1}{39} \frac{T}{5000} - 40, \quad (8)$$

$$\hat{\beta}_2 = \text{constant}, \quad 5000 \leq T \leq 200,000^\circ\text{K};$$

$$\hat{\beta}(T) = 1 + \left( \frac{T - 5000}{5000 a} \right)^{-1}, \quad (9)$$

$$a = \text{constant}, \quad 5000 \leq T \leq 10^6 \text{K},$$

where  $\hat{\beta}(T) \equiv \beta(T)/.16$  and  $T$  is measured in degrees Kelvin.

Equation (8) is a linear temperature relation for  $\hat{\beta}$  between the value of one at 5000°K to an arbitrary value  $\hat{\beta}_2$  at a higher temperature, arbitrarily chosen as 200,000°K. Hugoniot runs were made with  $\hat{\beta}_2$  taken as low as 0.1. The asymptotic approach of  $\hat{\beta}$  to zero in Eq. (9),  $T \rightarrow \infty$ ,  $\hat{\beta} \rightarrow 0$ , can be hastened or retarded by appropriate choices of the constant  $a$ . We have made Hugoniot calculations using Eq. (9) with values of  $a$  between 0.01 and 4.5. None of the p-v Hugoniot curves where Eqs. (8) and (9) were used exhibited sufficient departures from the corresponding Hugoniot based on  $\hat{\beta} = 1$  to account for the discrepancy between Thomas-Fermi and BKW Hugoniot results. It thus appeared that suitable alterations of curve (1), Fig. 3, could not be made by varying the parameter  $\beta$  over a reasonable range of values in Region II. This observation has led us to set  $\beta$  equal to 0.16 in the remainder of our investigations, and to focus our attention on constructing suitable functional forms for the parameter  $\kappa$  to achieve a smooth connection between the experimental and Thomas-Fermi Hugoniots of Fig. 2.

#### $\kappa$ AS A FUNCTION OF TEMPERATURE

Another possibility for obtaining smaller fluid volumes at a given pressure than those given by our constant-parameter Hugoniot is to allow the covolume factors to decrease with increasing pressure on the Hugoniot. Although this effect does occur already in our model via the temperature dependence of  $x$ , the covolume factors can be further decreased by varying  $\kappa$ , which appears as one of the products of the covolume factor terms in the definition of  $x$ .

Two possible variations of  $x$  have already been discussed, i.e.,  $\kappa(T)$  and  $\kappa(\bar{x})$ . We will first consider variations of  $\kappa$  with temperature.

In order to make the material softer,  $\kappa$  must decrease at the higher pressures. Since temperature increases with increasing Hugoniot

pressures, we must construct functions of temperature for  $\kappa$ , which give the correct value of 10.91 at a temperature of 5000°K, and decrease (but remain positive) for temperatures greater than 5000°K. An additional desirable condition would be to have the temperature derivative,  $\kappa'(T)$ , vanish at  $T = 5000^\circ\text{K}$ . The desirability of this follows from the appearance of  $\kappa'(T)$  in the equations of Appendix B. This condition has been relaxed because it had no significant effect on Hugoniot calculations on or near 5000°K. Computations were made with two different functional forms for  $\kappa(T)$ , both of which had nonzero values for  $\kappa'(5000^\circ\text{K})$ . The p-v Hugoniot solutions for these cases were essentially identical with the p-v Hugoniot based on constant  $\kappa$ , for temperatures between 5000°K and 15,000°K.

Two functional forms of  $\kappa(T)$  have been chosen. The normalized forms of these equations are

$$\hat{\kappa}(T) = \hat{\kappa}_2 + \frac{\hat{\kappa}_2 - 1}{39} \frac{T}{5000} - 40, \quad (10)$$

$$\hat{\kappa}_2 = \text{constant}, \quad 5000 \leq T \leq 200,000^\circ\text{K};$$

$$\hat{\kappa}(T) = 1 + \left( \frac{T - 5000}{5000 A} \right)^{-m}, \quad (11)$$

$$A, m = \text{constants}, \quad 5000 \leq T \leq 10^6^\circ\text{K},$$

where  $\hat{\kappa}(T) \equiv \kappa(T)/10.91$ , and  $T$  is again measured in degrees Kelvin.

Equation (10) has the same form as Eq. (8), and the parameter  $\hat{\kappa}_2$  may be interpreted in the same way; it is the value of  $\kappa$  at a temperature of 200,000°K. The primary reason for using Eq. (10) for  $\hat{\kappa}(T)$  was to ascertain whether reasonable variations in  $\kappa$  could be made to yield Hugoniot curves roughly in agreement with the Thomas-Fermi Hugoniot at pressures of approximately 20 megabars. Results of calculations using Eq. (10) are shown in Fig. 4. These results show that it is possible to obtain fair agreement with the Thomas-Fermi Hugoniot at the lower end of the Thomas-Fermi region, and that the value of the parameter  $\kappa$

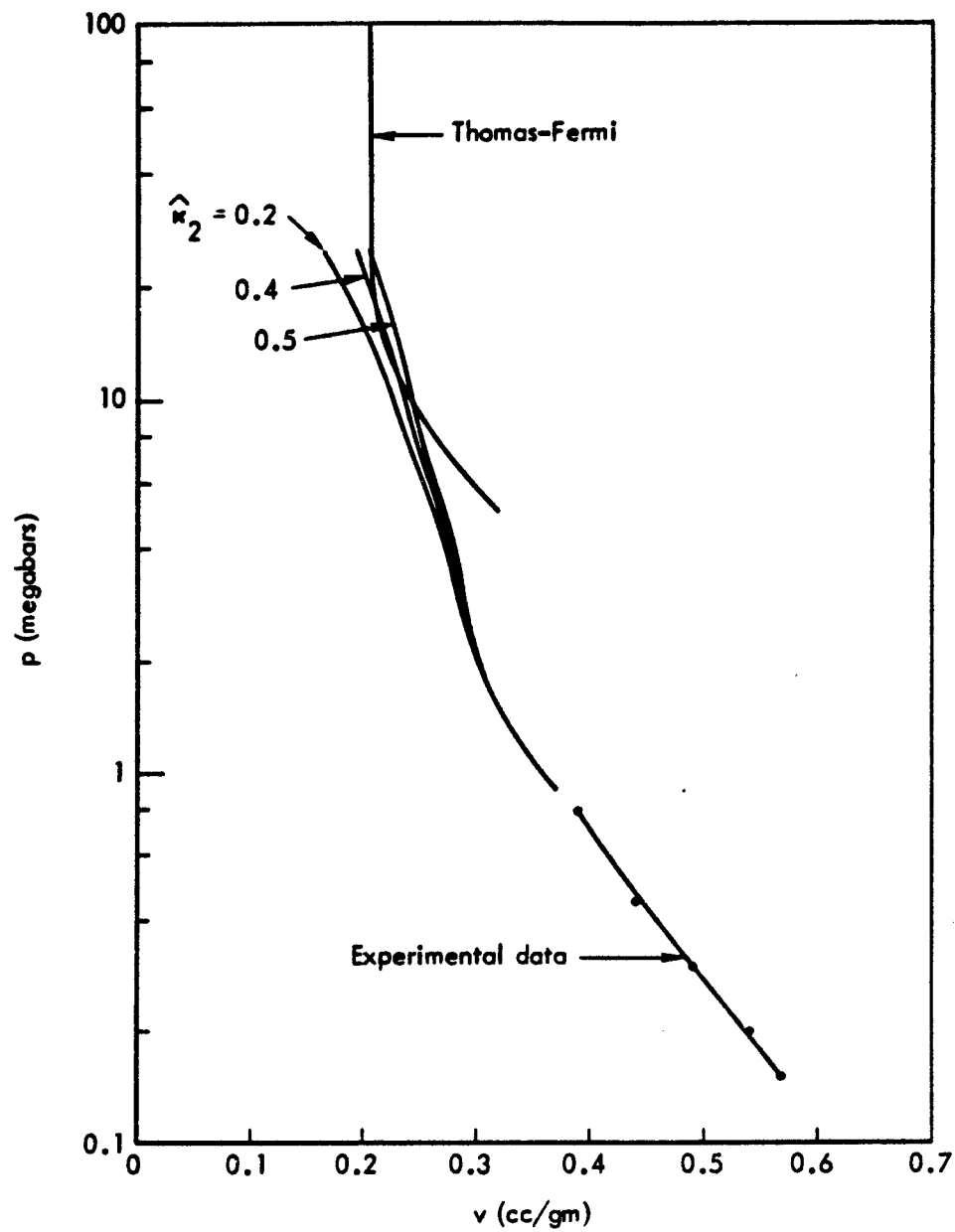


Fig.4—BKW Hugoniot curves, Region I;  $\kappa(T)$  from Eq. (10).

at 200,000°K must be reduced to approximately 40 percent of the value at 5000°K. The linear relation for  $\kappa(T)$  with  $\hat{\kappa}_2 = 0.4$  predicts negative values for  $\kappa$  at temperatures greater than approximately 330,000°K. This undesirable feature of Eq. (10) is not shared by Eq. (11), which was used for further computations.

The curves appearing in Fig. 5 were computed to obtain an estimate of the correct values that should be used for the parameters  $m$  and  $A$  in Eq. (11). The straight line in this figure represents the linear relation, Eq. (10), for  $\kappa(T)$ , with a value for  $\hat{\kappa}_2$  of .40. This particular value was chosen because it gave the best agreement between the Thomas-Fermi and BKW Hugoniot in Fig. 4. The remaining curves in Fig. 5 provide a sample of  $\kappa(T)$  relations obtained from Eq. (11), using various values for the parameters  $m$  and  $A$ . Approximate limits on the variation of  $A$  for a given  $m$  were obtained by requiring all eligible curves to go through a band,  $.40(1 - S_1) \leq \kappa(200,000) \leq .40(1 + S_2)$ , where the values of  $S_1$  and  $S_2$  are arbitrarily 1/2 and 1, respectively. Using this method and favoring those curves which lay nearer to the linear relation for temperatures between 5000°K and 200,000°K, we have chosen a value of 1 for  $m$ , and a set of  $A$ 's shown in Fig. 6.

Our final choice of parameters for  $\kappa(T)$  is  $A = 15$ ,  $m = 1$ , based on results shown in Fig. 6. The functional form of  $\kappa(T)$  which we therefore accepted as final is

$$\kappa(T) = \frac{10.91}{1 + \frac{T - 5000}{75,000}} \quad (12)$$

All remaining calculations, based on  $\kappa(T)$  both on and off the Hugoniot in Region I, will use this equation. Calculations off the Hugoniot are discussed in a later section.

#### $\kappa$ AS A FUNCTION OF $\bar{x}$

Before we can construct functions  $\kappa(\bar{x})$  that decrease with increasing Hugoniot pressures and temperatures, we must have some knowledge of how  $\bar{x}$  varies on the Hugoniot. No clear statement of  $\bar{x}$ 's variation

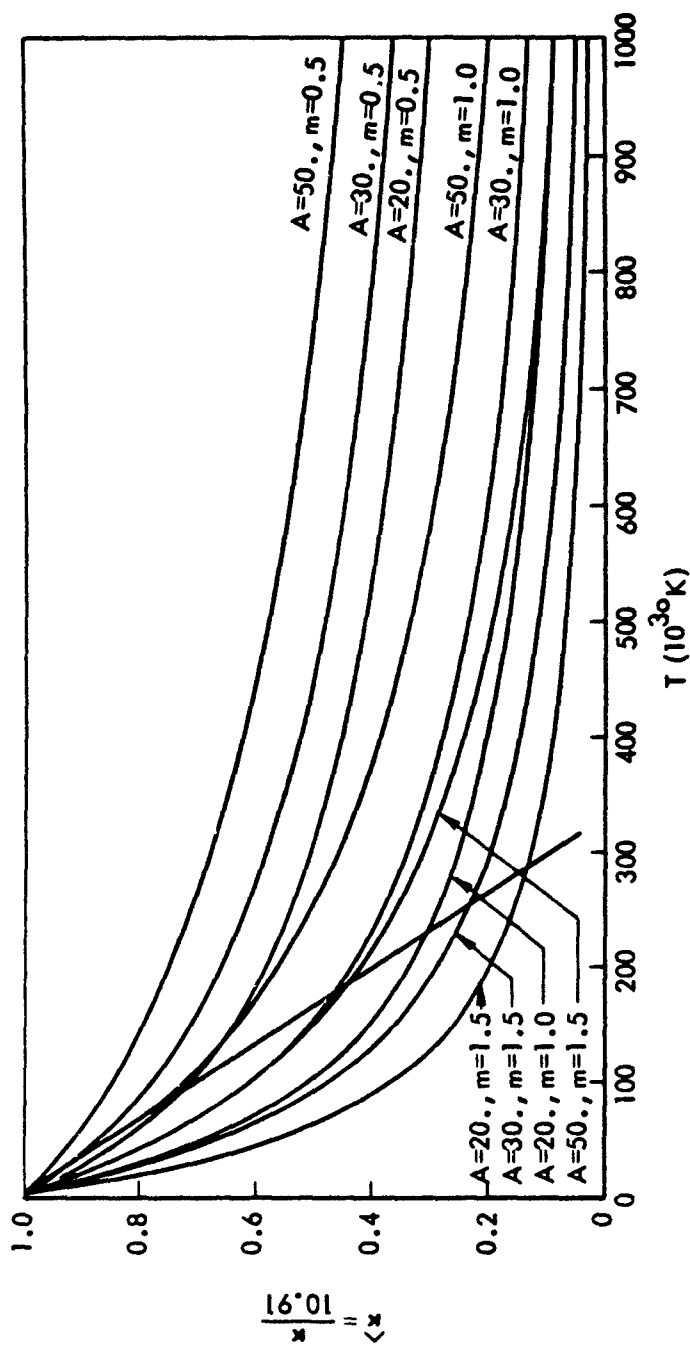


Fig. 5—Curves of  $\hat{\alpha}(T)$  versus  $T$ . Straight line is Eq. (10),  $\hat{\alpha}_2 = 0.4$ .

Remaining curves correspond to Eq. (11).

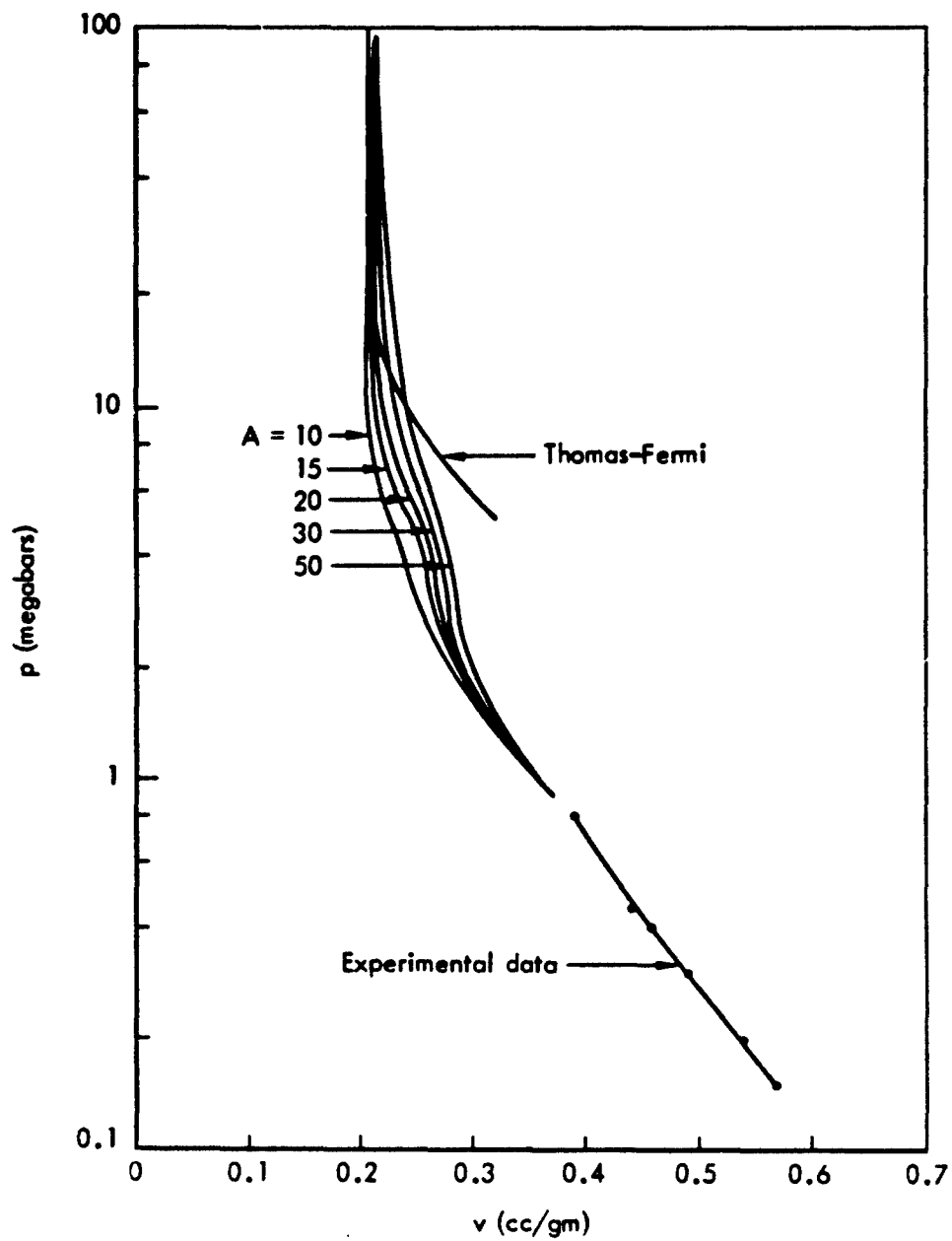


Fig. 6—BKW Hugoniot curves, Region I;  $\hat{\kappa}(T)$  from Eq. (11),  $m = 1$ .

on the Hugoniot can be made directly from its definition,

$$\bar{x} = \frac{\sum_{i=1}^{23} n_i k_i}{V(T + \theta)^\alpha},$$

for while  $V$  decreases with increasing  $p$ ,  $(T + \theta)^\alpha$  increases, and the variations of the numerator are unpredictable without extensive calculation.

Some insight into  $\bar{x}$ 's variation can be obtained from the results of Hugoniot calculations shown in Table 5. These results are based on constant values for all of the parameters (Mader's recommended values for  $\alpha$ ,  $\beta$ ,  $\kappa$ ,  $\theta$ , and the first set of covolume factors in Table 4). In Table 5,  $\bar{x}$  on the Hugoniot decreases monotonically toward zero with increasing pressure (and temperature). Because these results are based on constant  $\kappa$ , they are only an indication of the behavior of  $\bar{x}$  for variable  $\kappa$ . However, they are sufficient to establish reasonable trial forms for  $\kappa(\bar{x})$ . Trial forms are therefore chosen to vanish at  $\bar{x} = 0$ , to give the correct value of  $\kappa = 10.91$  at  $T = 5000^\circ\text{K}$  on the Hugoniot (where  $\bar{x} = 0.50566$  from Table 6), and to increase monotonically with  $\bar{x}$  for  $\bar{x} > 0$ .

Of the various forms tried, the following simple expression most successfully matches Hugoniot curves to the Thomas-Fermi Hugoniot at high pressures:

$$\hat{\kappa}(\bar{x}) = \left( \frac{\bar{x}}{0.50566} \right)^\gamma, \quad (13)$$

$$\bar{x} > 0, \quad \gamma = \text{constant},$$

where  $\hat{\kappa}(\bar{x}) \equiv \kappa(\bar{x})/10.91$ .

Calculations based on Eq. (13) used in association with the relations of Appendix C are presented in Fig. 7, which is a set of  $p$ - $v$  Hugoniot curves parameterized on  $\gamma$ . From Fig. 7, we have chosen the

Table 6

HUGONIOT CALCULATIONS BASED ON FIRST SET OF PARAMETERS, TABLE 5  
COVOLUME FACTORS FROM SET 1 OF TABLE 4

$T(^{\circ}\text{K}) \times 10^{-3}$	$p(\text{megabars})$	$\bar{x}$
5	0.887	0.50566
7	1.23	0.475
10	1.60	0.425
15	2.23	0.365
20	2.85	0.311
30	4.50	0.205
50	6.50	0.139
70	8.39	0.113
100	11.34	0.0909
150	17.15	0.0698
200	24.12	0.0574
300	40.15	0.0420
500	78.20	0.0270
700	119.1	0.0196
1000	189.4	0.0132

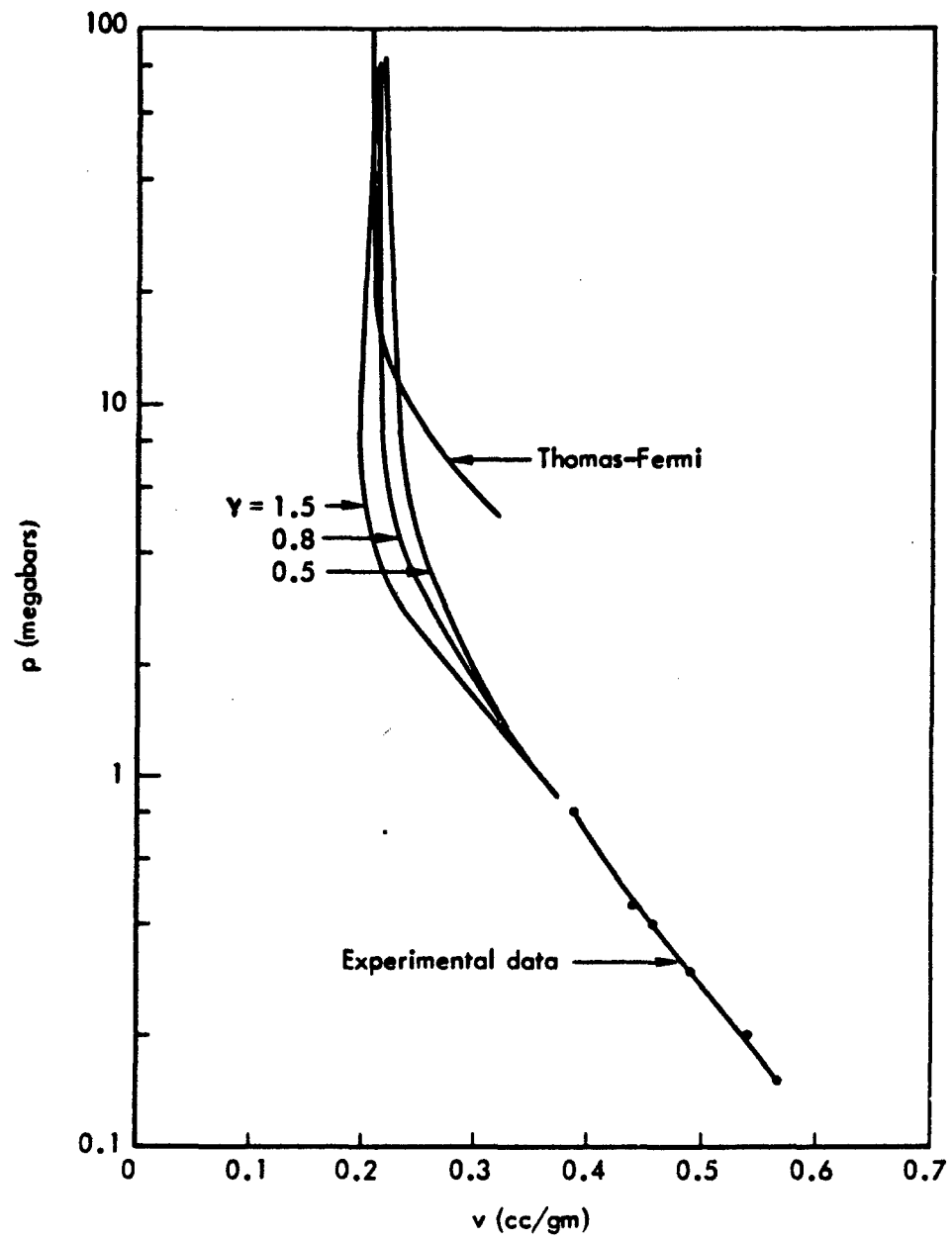


Fig.7—BKW Hugoniot curves, Region I;  $\kappa(\bar{x})$  from Eq. (13).

value of  $\gamma$  equal to 0.8. All subsequent calculations using  $\kappa(\bar{x})$  will incorporate

$$\kappa(\bar{x}) = 10.91 \left( \frac{\bar{x}}{0.50566} \right)^{0.8} . \quad (14)$$

## VI. RESULTS ON ISOTHERMS AND ISOMETRICS, REGION I

Table 5 contains a summary of the parameters used for the three sets of computations [ $\kappa = \text{constant}$ ,  $\kappa = \kappa(T)$ ,  $\kappa = \kappa(\bar{x})$ ] in the remainder of this Report.

Pressure-volume-temperature calculations for a set of isotherms spanning the low-pressure part of the Thomas-Fermi region are compared to the corresponding Thomas-Fermi isotherms in Figs. 8, 9, and 10, where each figure employs a different set of the parameters appearing in Table 5. Energy-volume-temperature comparisons are made in Figs. 11, 12, and 13 on the same set of isotherms that appear in the p-v-T diagram.

The p-v-T comparisons of Figs. 8, 9, and 10 are somewhat surprising, because the solutions for the constant- $\kappa$  set of parameters, which gave the worst p-v Hugoniot results, match the p-v isotherms of the Thomas-Fermi model better than do the variable- $\kappa$  cases, whose pressures on isotherms are consistently lower than the corresponding Thomas-Fermi pressures. However, the e-v-T comparisons shown in Figs. 11, 12, and 13 yield consistently low BKW energies on isotherms for all three sets of parameters. Comparison of p-v-T and e-v-T results for each set of calculations suggests that the variable- $\kappa$  cases might yield better p-v-e results than the constant- $\kappa$  case, since such results are the temperature eliminant of the p-v-T and e-v-T calculations in Figs. 8 to 10 and 11 to 13, respectively. This does indeed turn out to be true, as can be seen in Figs. 14, 15, and 16. In these figures, the BKW p-e curves corresponding to four isometrics spanning the low-pressure Thomas-Fermi region come much closer to the corresponding Thomas-Fermi isometrics for the variable- $\kappa$  calculations. This last set of results is consistent with the p-v Hugoniot results presented earlier, for p-v Hugoniot calculations use only the pressure-volume-energy form of the equation of state. Thus, the variable  $\kappa$ 's chosen to fit known p-v Hugoniot results were tailored to favor a correct form of the p-v-e relation.

Since our equation of state will be primarily used in hydrodynamic calculations, which mainly use the p-v-e form, we base our final choice of parameters on the comparisons appearing in Figs. 14 to 16. In these figures, the  $\kappa(T)$  and  $\kappa(\bar{x})$  calculations yield essentially the same

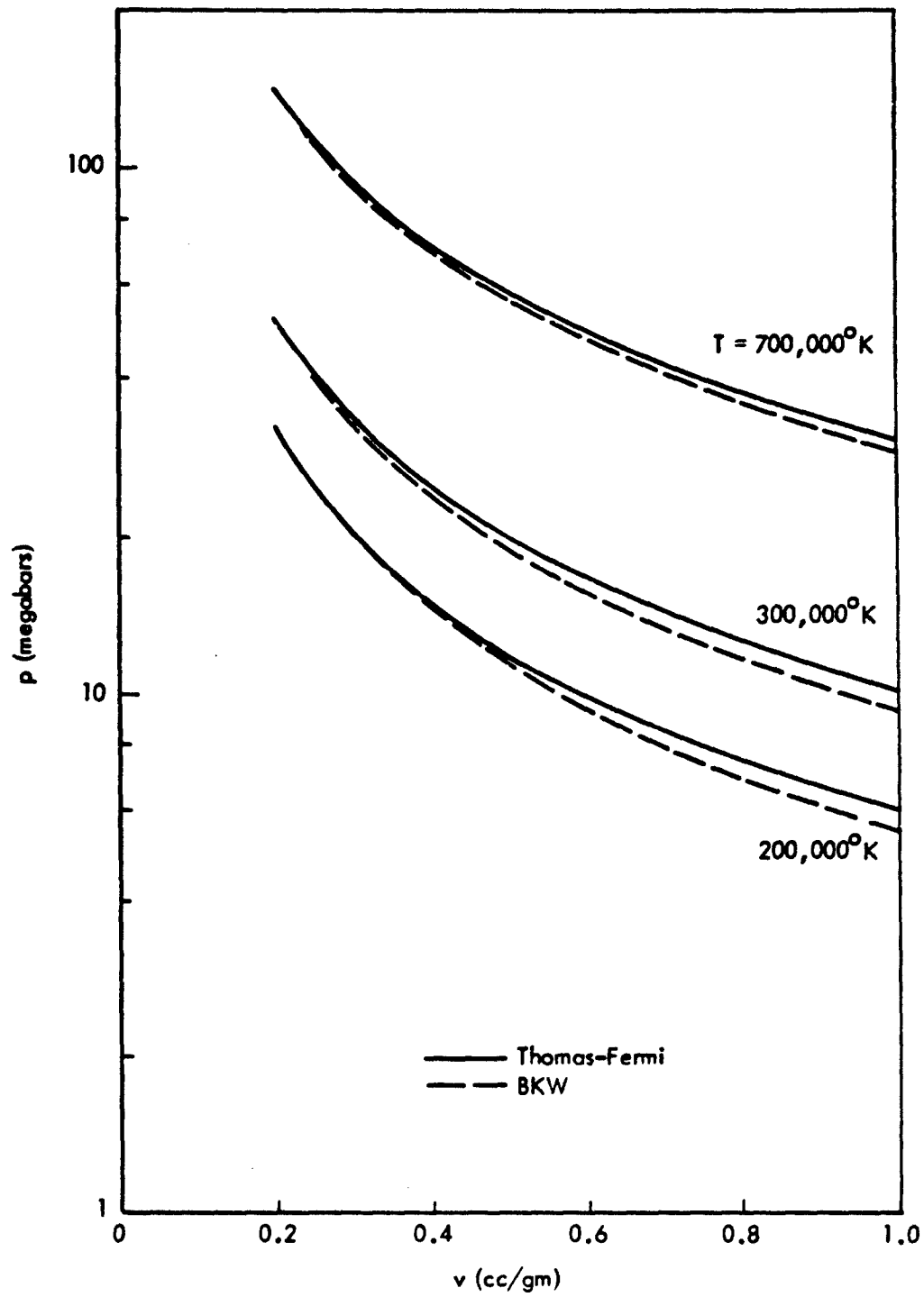


Fig.8—Thomas-Fermi and BKW  $p$ - $v$  isotherms, Region I. BKW results are based on  $\kappa = 10.91$ .

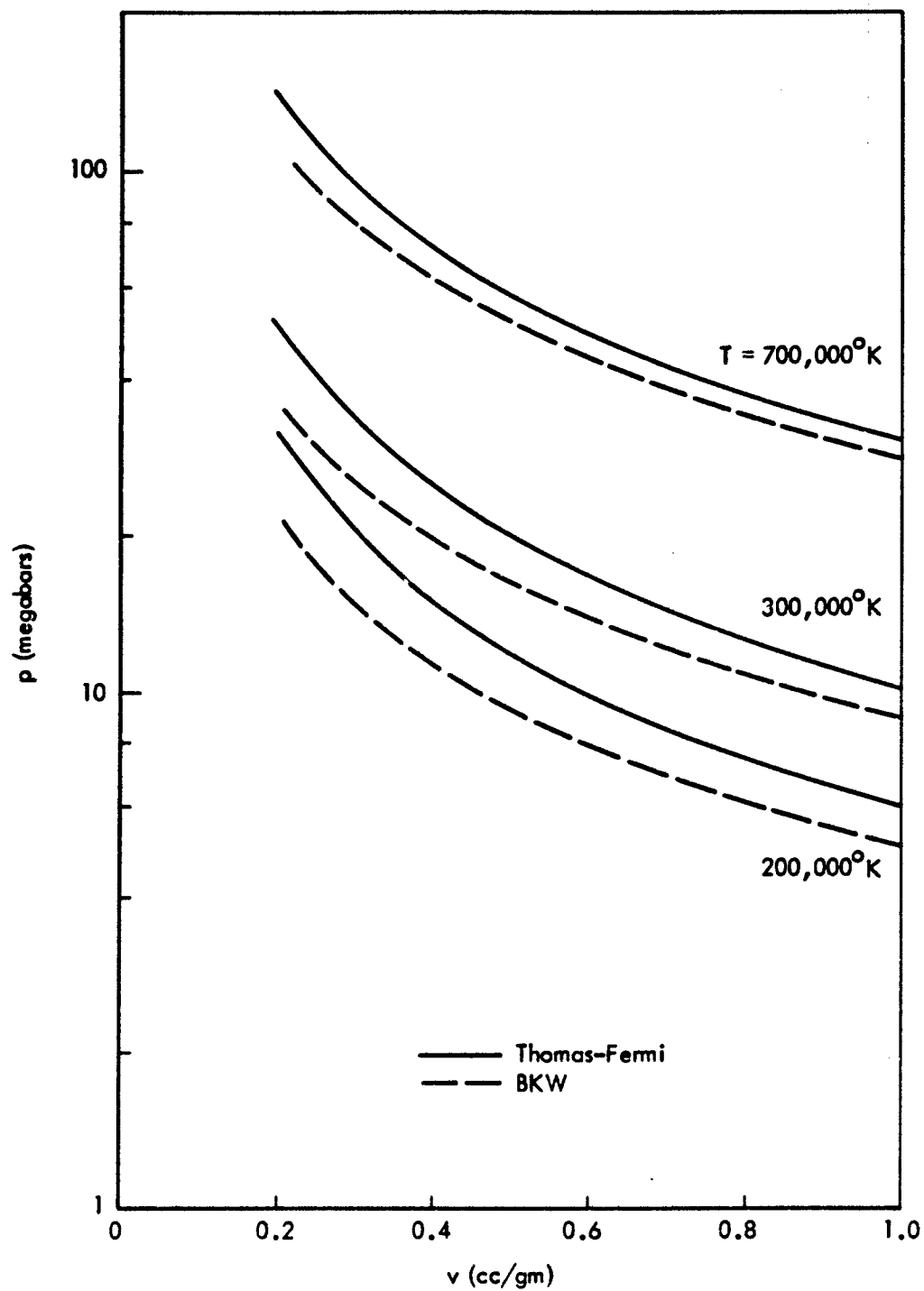


Fig.9—Thomas-Fermi and BKW  $p$ - $v$  isotherms, Region I. BKW results are based on  $\kappa(T)$  given by Eq. (12).

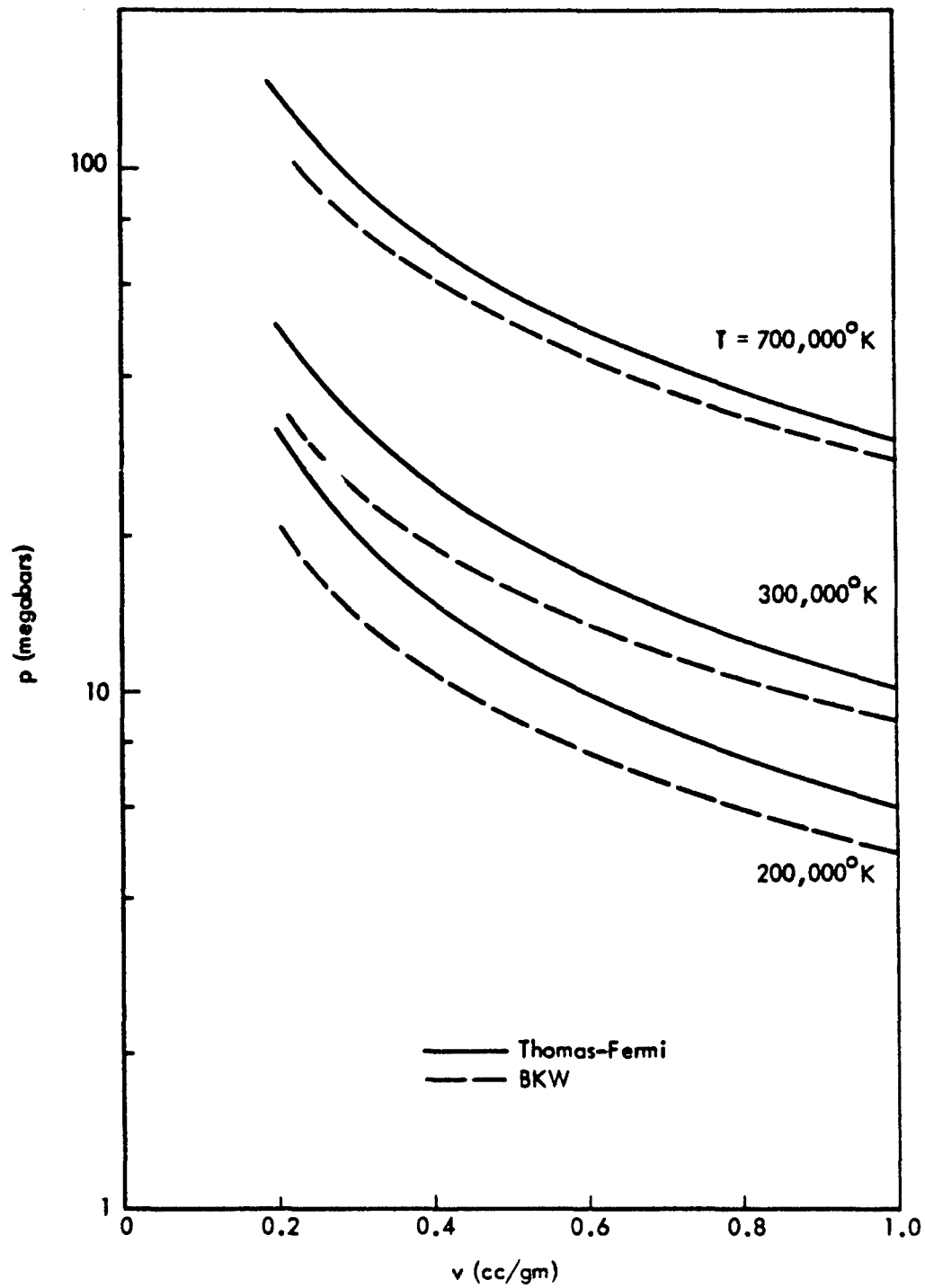


Fig.10—Thomas-Fermi and BKW  $p$ - $v$  isotherms, Region I. BKW results are based on  $\kappa(\bar{x})$  given by Eq. (14).

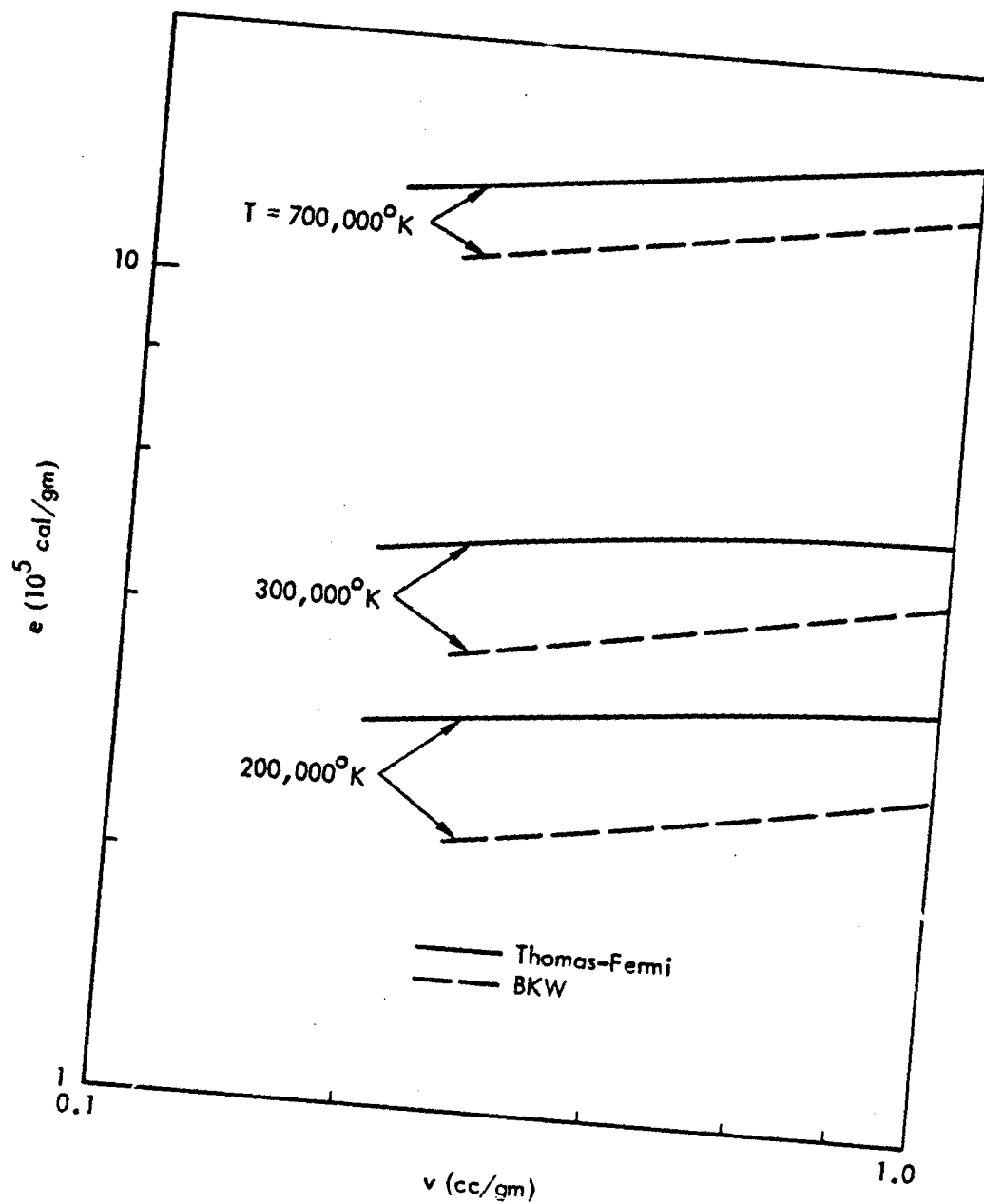


Fig. 11—Thomas-Fermi and BKW  $e$ - $v$  isotherms, Region I. BKW results based on  $\kappa = 10.91$ .

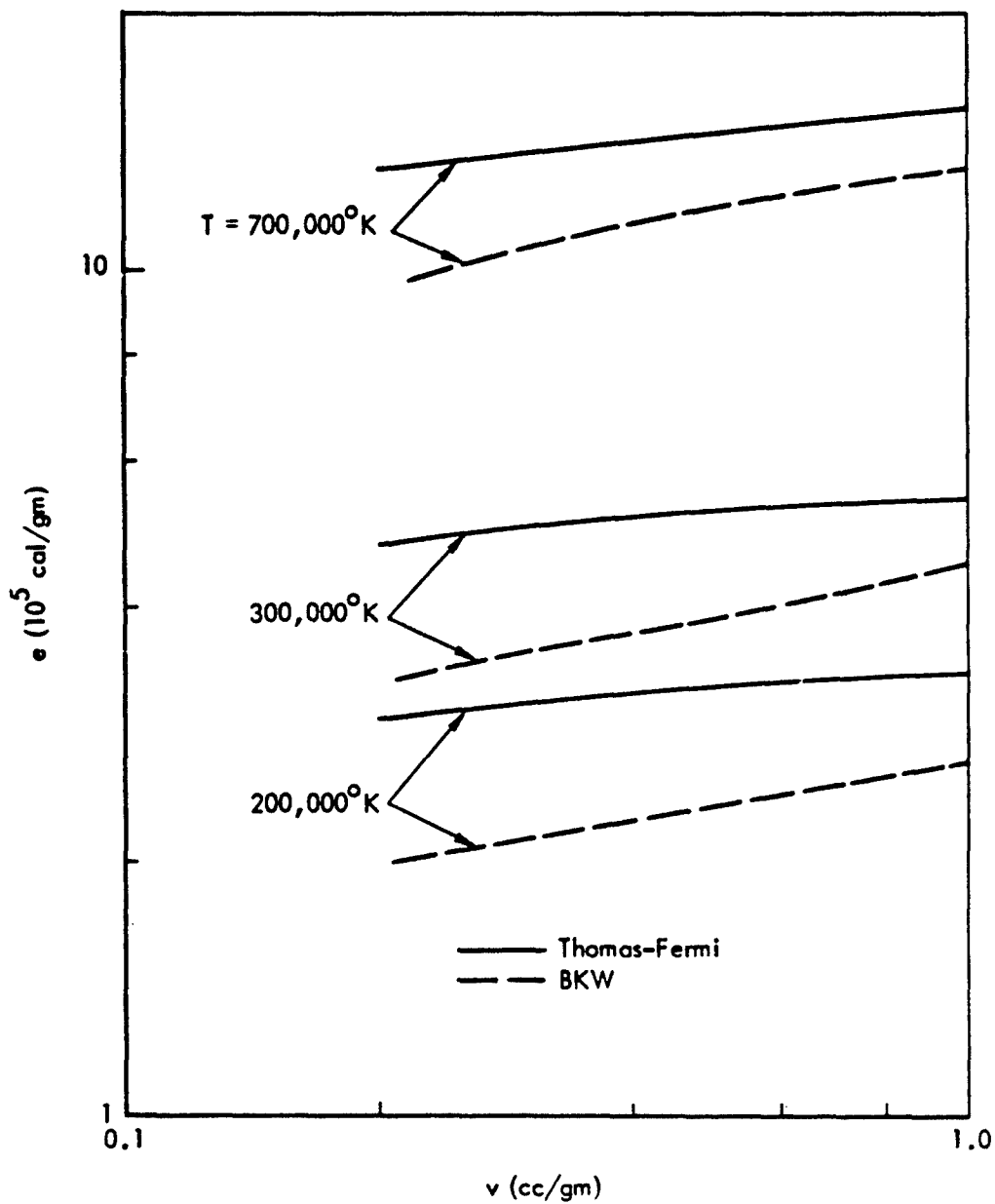


Fig.12—Thomas-Fermi and BKW  $e$ - $v$  isotherms, Region I. BKW results are based on  $\kappa(T)$  given by Eq. (12).

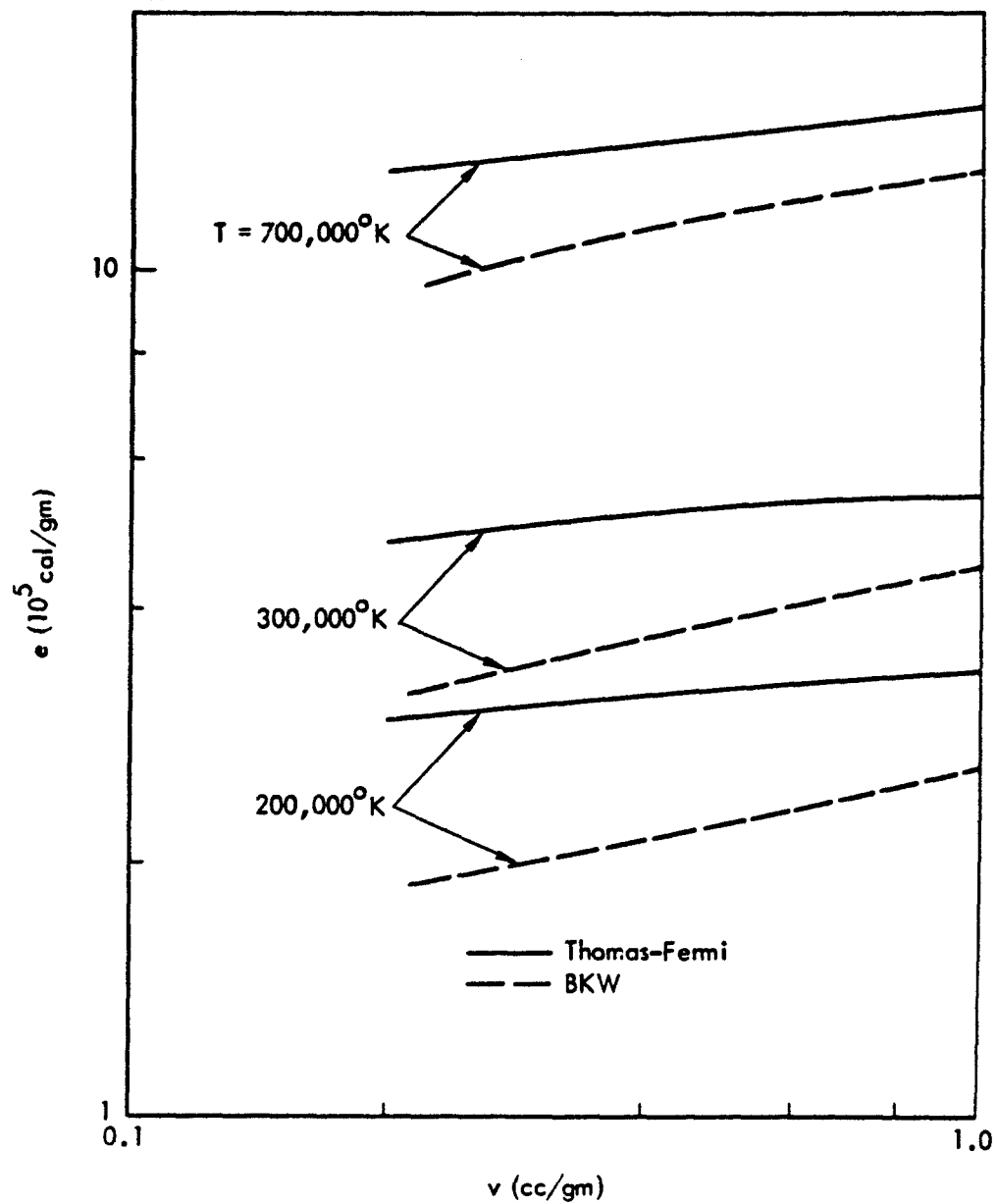


Fig. 13—Thomas-Fermi and BKW  $e$ - $v$  isotherms, Region I. BKW results are based on  $\kappa(\bar{x})$  given by Eq. (14).

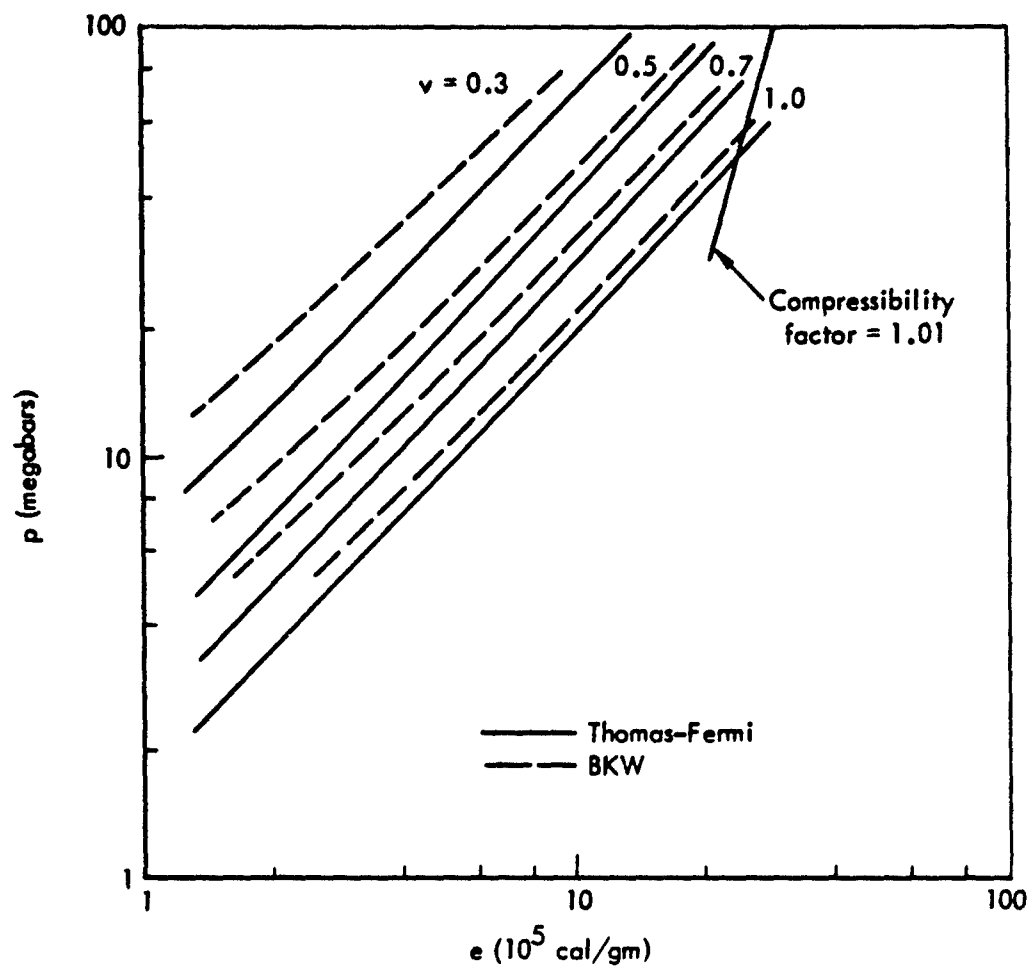


Fig. 14—Thomas-Fermi and BKW  $p$ - $e$  isometrics, Region I.  
BKW results are based on  $\kappa = 10.91$ .

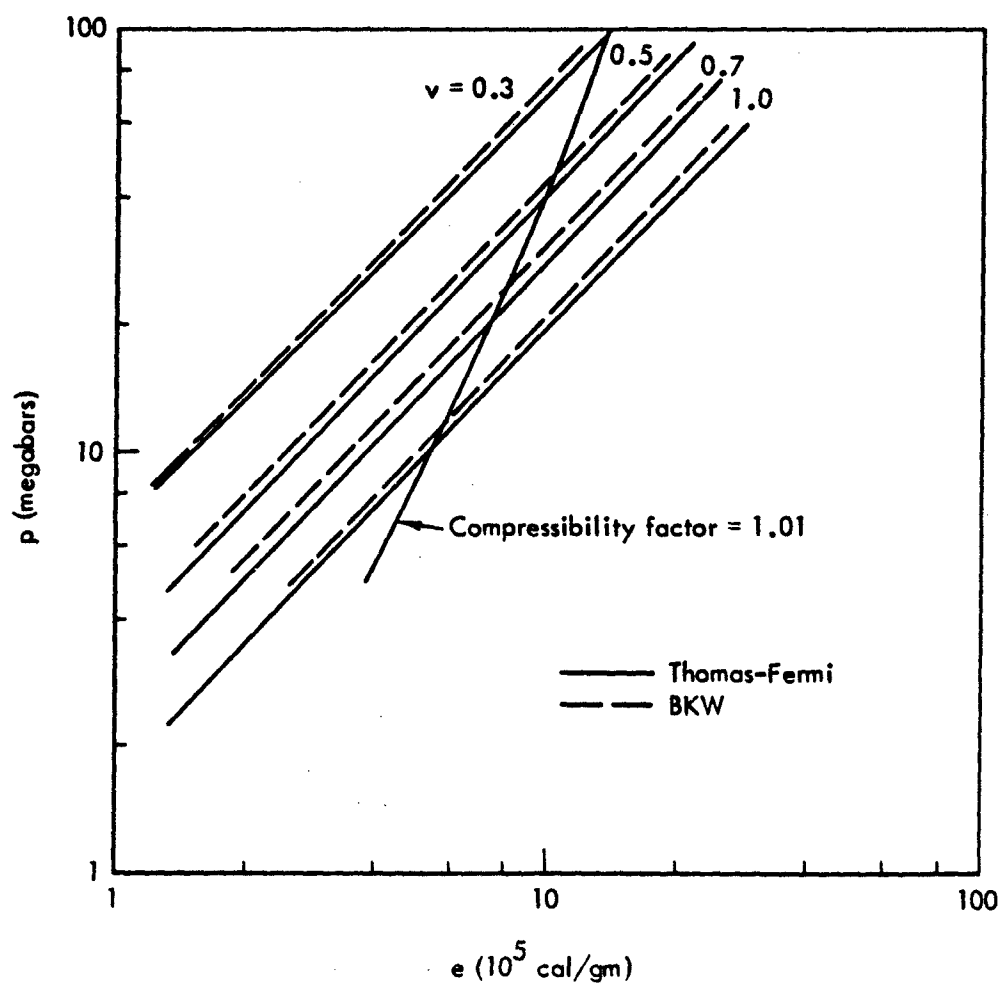


Fig. 15—Thomas-Fermi and BKW  $p$ - $e$  isometrics, Region I. BKW results are based on  $\kappa(T)$  given by Eq. (12).

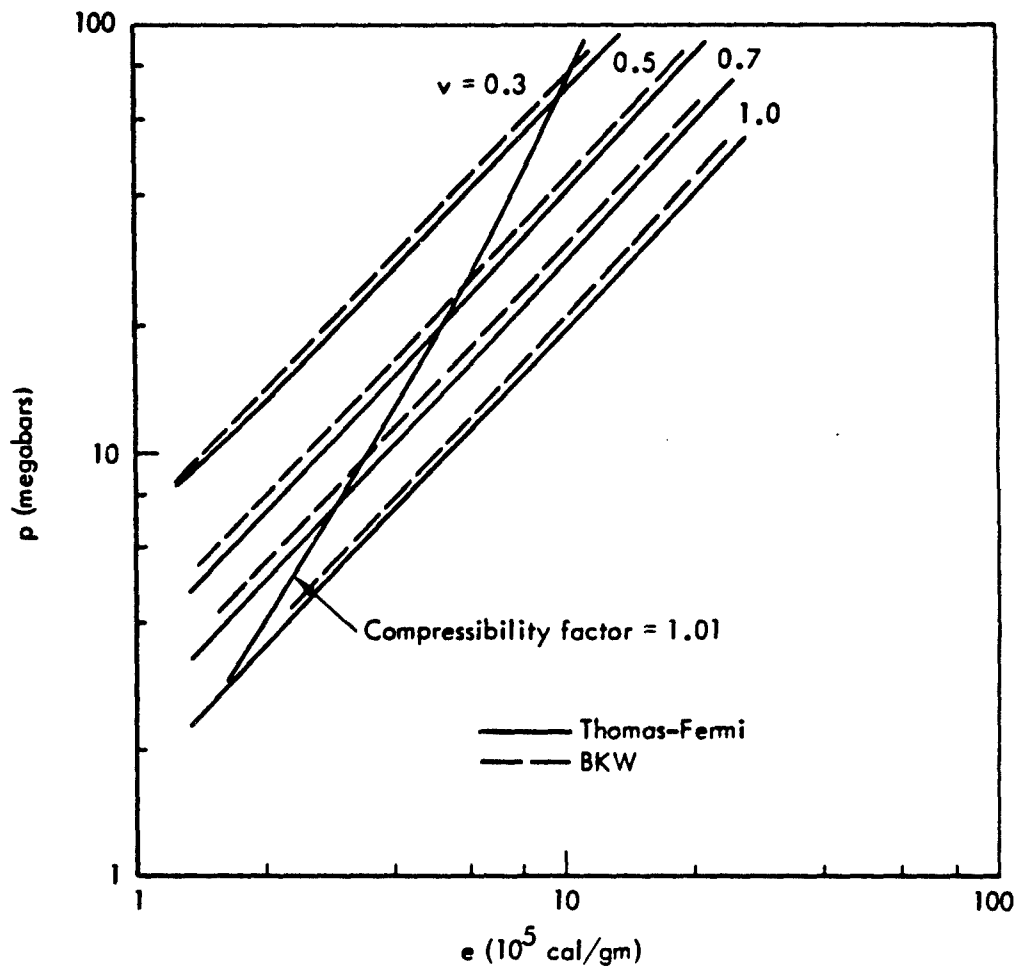


Fig.16—Thomas-Fermi and BKW  $p$ - $e$  isometrics, Region II.  
BKW results are based on  $\kappa(\bar{x})$ , Eq. (14).

result. Both predict pressures that are consistently higher, by approximately 7 percent, than the Thomas-Fermi solution at the same energy and volume.

We choose the  $\kappa(T)$  parameters (set 2 of Table 5) to represent the p-v-e results of this Report in Region I, since the  $\kappa(T)$  calculations on isotherms agreed a little better than the  $\kappa(\bar{x})$  calculations with Thomas-Fermi results.

Because of the generally poor performance of the variable- $\kappa$  isothermal calculations and the equally poor constant- $\kappa$  p-v-e (and Hugoniot) results, we will not present detailed p-v-T or even e-v-T results in Regions I and II based on the BKW equation or any of its modifications considered here. Detailed pressure-volume-energy results are presented later in Fig. 21.

## VII. HUGONIOT CALCULATIONS, REGION II

Hugoniot calculations with all three sets of parameters appearing in Table 6 showed that at 5000°K and 7000°K there were insignificant traces of all species other than  $H_2O$ . Thus, below 5000°K, the Hugoniot calculations were based on pure water. This is not true however, for p-v points off of the Hugoniot. Off of the Hugoniot, the six species  $H$ ,  $O$ ,  $H_2$ ,  $O_2$ ,  $H_2O$ , and  $OH$  were assumed to exist in chemical equilibrium in Region II. Another simplification occurring in Region II stems from the fact that its pressure range, which runs from about 0.5 to 1 megabar, approximately coincides with a large part of the range of pressures over which the BKW parameters of Ref. 14 were established. Hugoniot calculations were made using these parameters (set 1, Table 5, and the  $k_1$  of set 1, Table 4), in association with standard state data given at 100°K increments from 100°K to 6000°K.<sup>†</sup> The p-v Hugoniot curve obtained from these calculations is placed on Fig. 17, which is a partial reproduction of Fig. 1, Ref. 14. The results of our Hugoniot calculations can be seen to be in good agreement with those of Ref. 14 above approximately .2 megabar, with minor discrepancies that can be attributed to differences in standard state data and ambient temperatures at the foot of the Hugoniot between our calculations and those of Ref. 14. Below approximately .17 megabar the BKW equation predicts shock temperatures lower than the ambient temperature of the unshocked material. This renders comparisons between our results and those of Ref. 14 somewhat meaningless below .17 megabar, since in this region the results of either set of calculations represent physical nonsense.

Although the p-v Hugoniot results using the BKW method exhibit fairly good agreement with experimental data, the p-T Hugoniot calculations lead to results that in our opinion do not bear even a casual relation to the p-T Hugoniot data for water. This observation is based on a comparison of the experimental and BKW p-T Hugoniot curves shown in Fig. 18. The results of Fig. 18 place considerable doubt on the

---

<sup>†</sup>See Ref. 24 for standard state data below 6000°K.

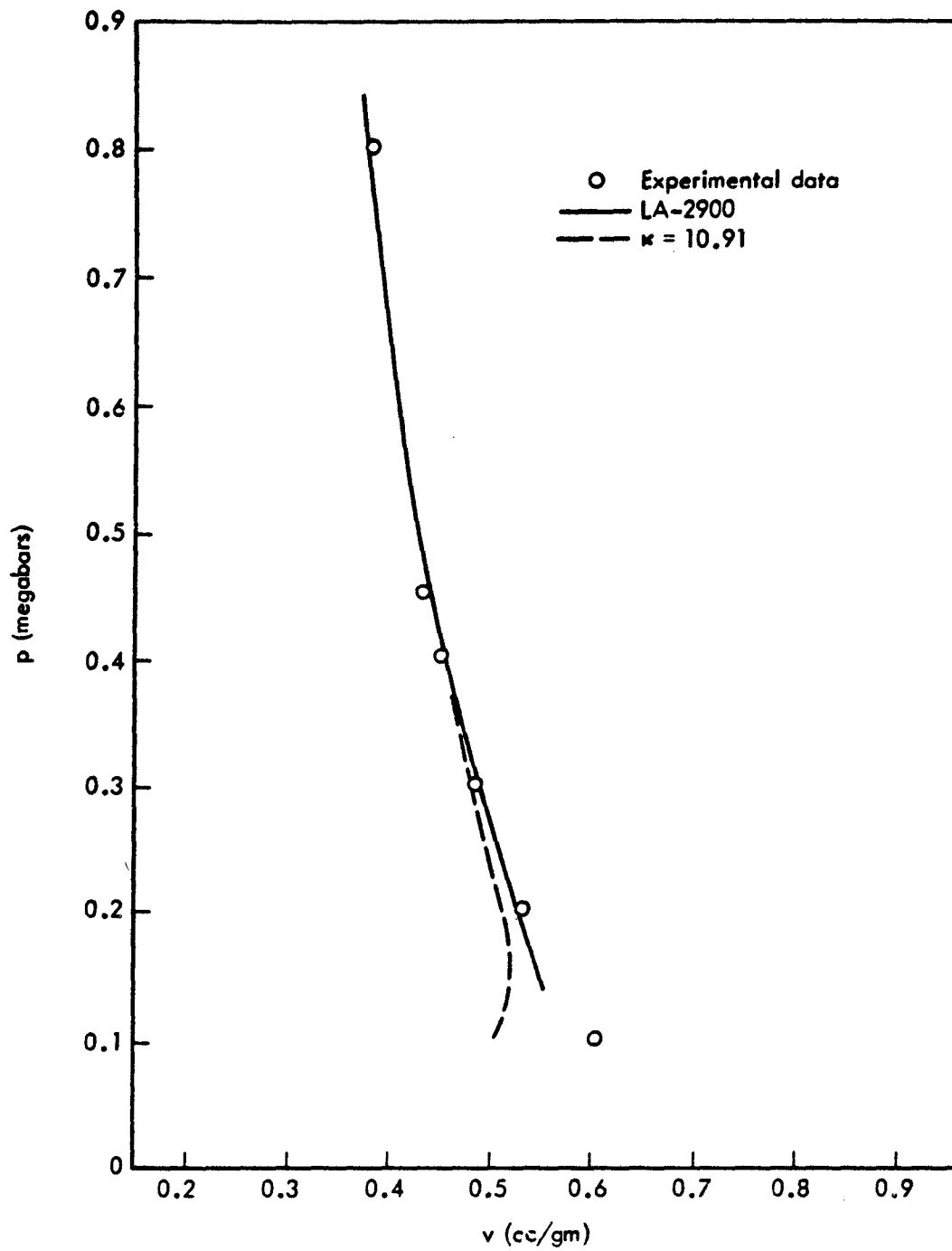


Fig.17—8KW Hugoniot curves, Regions II and III. Solid and dashed curves are based on first set of parameters (Table 6), with  $k_{14} = 250$ .

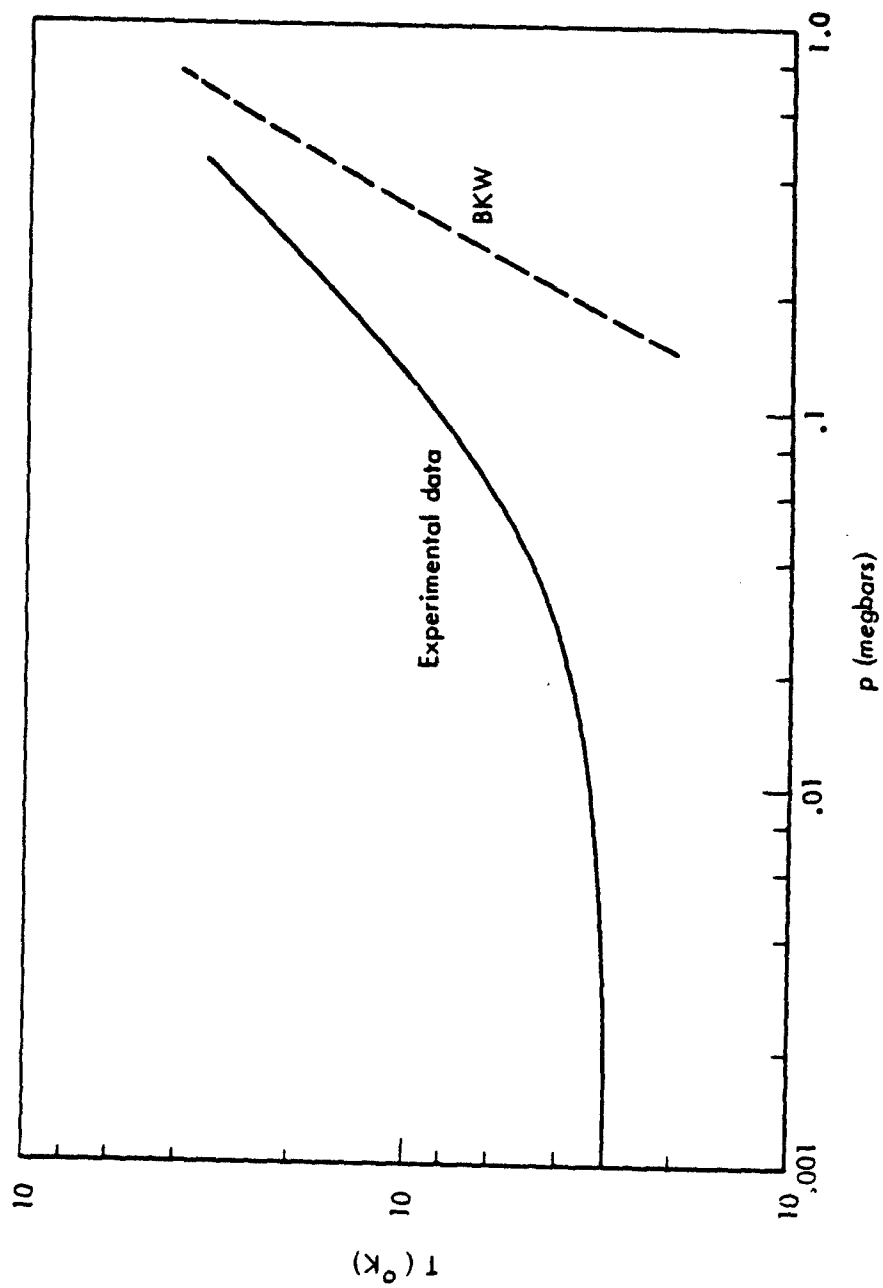


Fig. 18—Comparison of BKW p-T Hugoniot curve, Regions II and III, with that of experimental data.

value of the temperature-dependent BKW equations for representing the equilibrium properties of water near the Hugoniot at pressures above .1 megabar. This conclusion is supported by the results of the following section.

# VIII. RESULTS ON ISOTHERMS AND ISOMETRICS, REGION II

In Region II it is difficult to obtain a good evaluation of BKW results on isotherms and isometrics at pressures above .25 megabar and for temperatures higher than a few thousand degrees Kelvin, since reference curves are difficult to obtain in these regions. The best that we can do is to extrapolate the results of Rice and Walsh to higher temperatures and pressures than were incorporated in their work.<sup>(4)</sup> For the p-v isotherms, we use the results of Ref. 8 as reference curves. These results, however, represent an extrapolation of one of the assumptions of Ref. 4,  $(\partial v / \partial T)_p = f(p)$ , to temperatures as high as 10,000°K. No justification of this assumption appears in the text of Ref. 8. For p-e comparisons on isometrics, we obtain reference curves to .450 megabar by extrapolating the curve fit of Ref. 4 for the quantity  $(\partial h / \partial v)_p = \xi(p)$ , to pressures of .450 megabar. In Ref. 4, this expression is terminated at a maximum pressure of .250 megabar. The rather uncertain value of these extrapolations leads us to make comparisons only in a small neighborhood of the Hugoniot curve above .250 megabar, since the extrapolations are more reliable near the Hugoniot than anywhere else.

In Region II as in Region I, the BKW equation exhibits a poor temperature performance, as is clearly borne out by Fig. 19. This figure compares the BKW p-v-T solutions based on the first set of parameters of Table 5 with the results of Ref. 8. These results, along with equally unflattering comparisons of the BKW e-v isotherms with reference curves (not shown) has led us to conclude that in Region II as well as in Region I, the BKW method does not yield acceptable p-v-T and e-v-T equations of state near the Hugoniot curve.<sup>†</sup>

Pressure-energy isometrics are shown in Fig. 20 for both the reference and BKW systems. A comparison of the reference and BKW isometrics of Fig. 20 has led us to reject the BKW p-v-e results at pressures lower than approximately .3 megabar.

<sup>†</sup>Reference isotherms and isometrics have also been obtained from the more recent results of Ref. 25. Comparisons of the BKW curves of Figs. 19 and 20 with these later results have not produced any changes in the conclusions and recommendations of this Report.

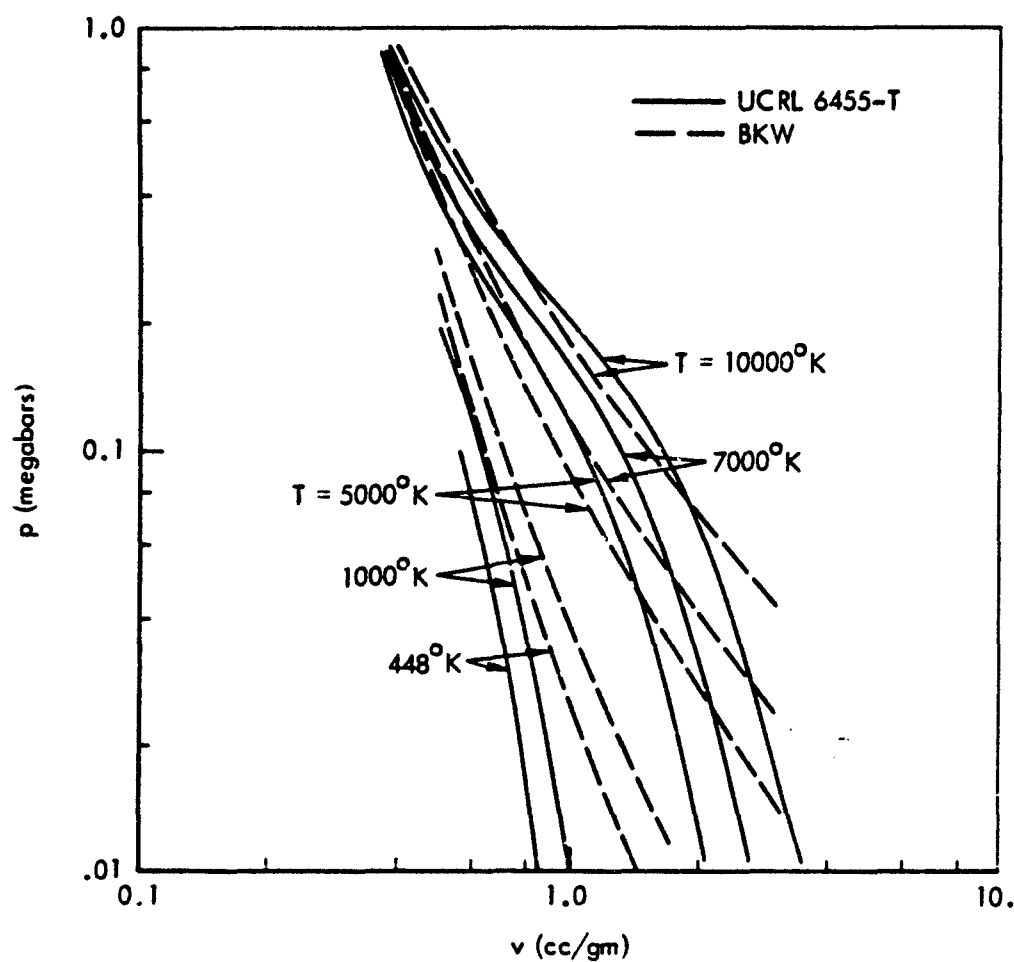


Fig. 19—Comparison of BKW  $p$ - $v$  isotherms, Region II, with those of Ref. (18).

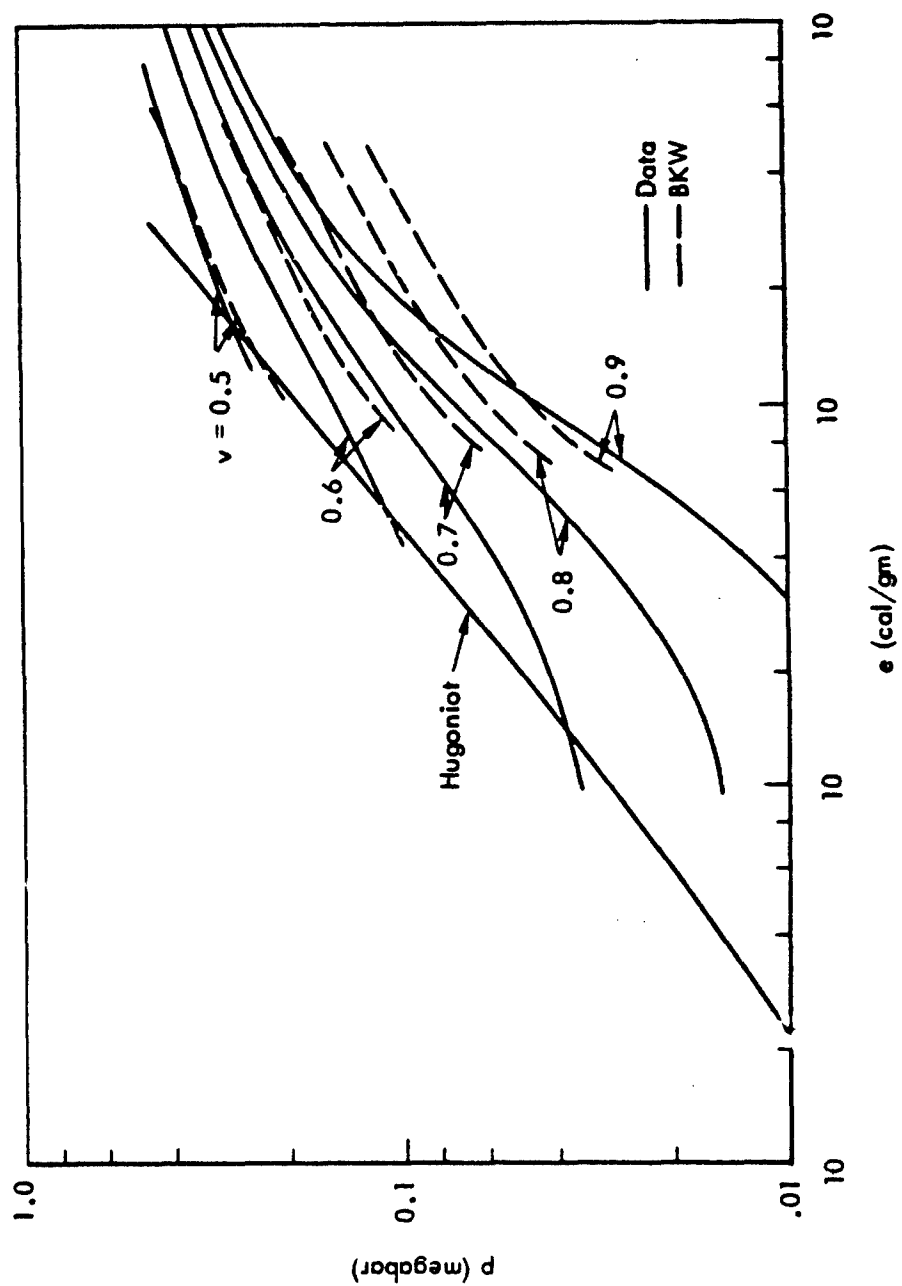


Fig. 20—Comparison of BKW p-e isometrics, Region II, with those Ref. (4).

### IX. SUMMARY OF RESULTS AND DISCUSSION

1. Our studies have shown that the unmodified forms of the BKW equation are generally unsatisfactory near the Hugoniot. In particular, the p-T Hugoniot curve predicted by the BKW method is completely in error. However, results on p-v isotherms above 200,000°K suggest that the unmodified form of the BKW p-v-T relation is satisfactory above this temperature if the parameters of Ref. 13 are used.

2. Of the modifications attempted, only those that altered the covolume factors of the mixture showed any appreciable tendency to bring the p-v Hugoniot back into line with the known Thomas-Fermi results. Both of the trial forms for variable covolume factor [ $\kappa(\bar{x})$  and  $\kappa(T)$ ] produced satisfactory p-v Hugoniot results. In each case this was accomplished by forcing the modified forms of the BKW equation to lie closer to the ideal-gas equation of state than does the unmodified form.

3. The modified BKW forms produced unsatisfactory p-v-T and e-v-T results at temperatures as high as 700,000°K, except in the ideal-gas range. However, the modified forms (in particular the form where  $\kappa$  assumed a dependence upon temperature) produced reasonable p-v-e results above approximately 300 kilobars for the region lying between the Hugoniot curve and the 10,000 megabar-adiabat.

4. The combined p-v-e results of Regions I and II are presented in Fig. 21. Results have been altered slightly so that they smoothly join the Thomas-Fermi solutions of Ref. 2, which also appear in Fig. 21. The dashed lines represent linear extrapolations of computed isometrics (solid lines). The figure also includes the Hugoniot curve and the 10,000-megabar adiabat (the isentrope through the Hugoniot at a pressure of  $10^4$  megabars). These curves represent the approximate boundaries of the region required for nuclear burst calculations in water.<sup>†</sup> The 10,000-megabar adiabat was obtained by numerically integrating the relation  $de = -pdv$ , with the aid of the p-v-e results of Fig. 21, from the 10,000-megabar point on the Hugoniot.

<sup>†</sup>See Ref. 1 for a discussion of the approximate range requirements for nuclear burst calculations.

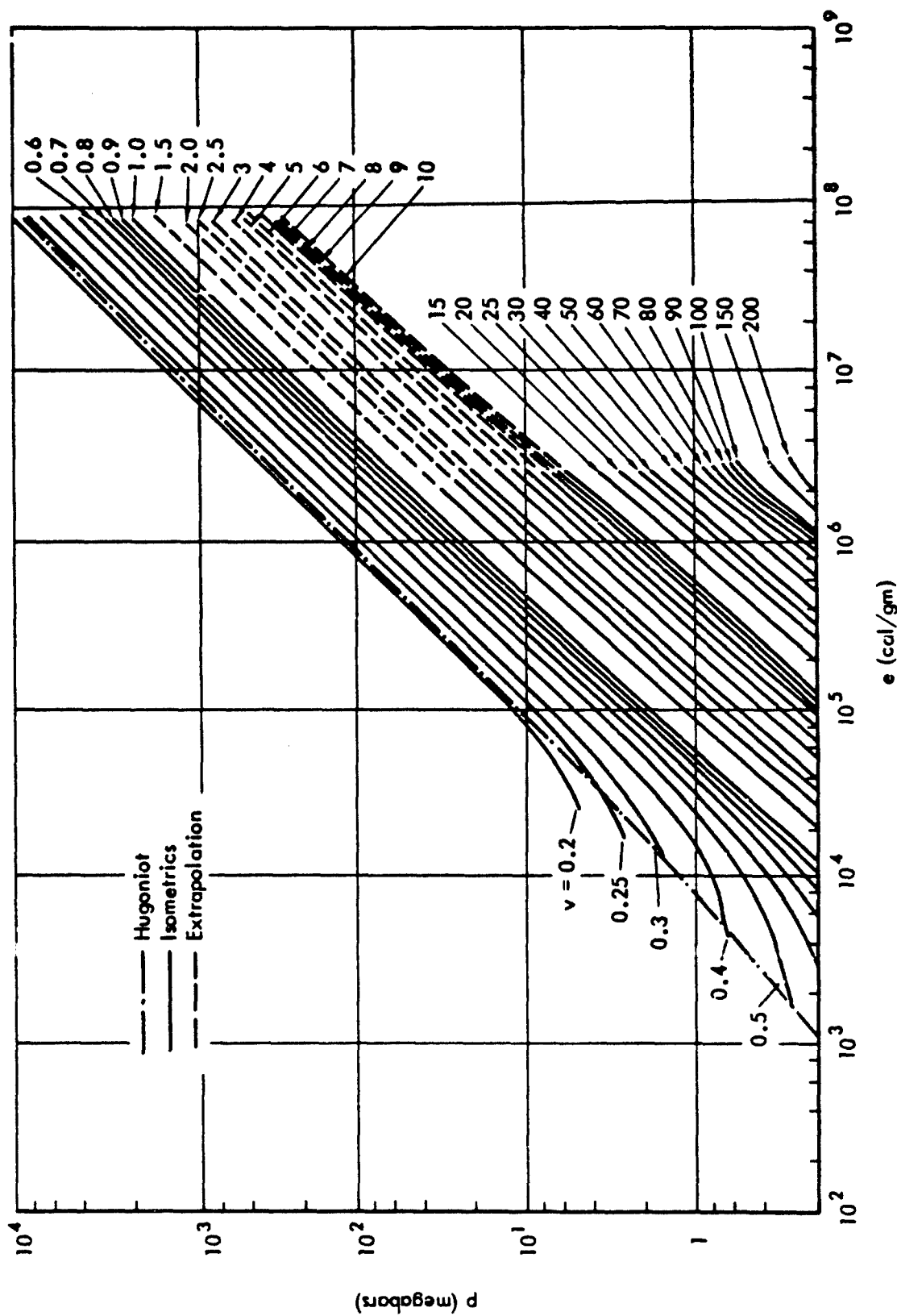


Fig.21—Pressure-volume-energy relation for water above 300 kilometers

We regard the  $p-v-e$  results obtained here as somewhat unsatisfactory, but perhaps as good as could reasonably be provided by the BKW form of the thermal equation of state. Any further improvement in the combined  $p-v-T$ ,  $e-v-T$ , and  $p-v-e$  relations will simply require a more satisfactory point of departure (thermal equation of state, partition function, etc.) than is offered by the BKW equation.

# Appendix A

## SUMMARY OF THERMODYNAMIC RELATIONS BASED ON THE THERMAL (p,V,T) EQUILIBRIUM EQUATIONS

In this summary, the distinction between ideal gas and residual contributions to the various quantities appearing is retained wherever it is reasonable to do so. The pertinent equations are:

$$p = p(T, V, \underline{n}) \quad (A-1)$$

$$E = \sum_{i=1}^c n_i [\bar{H}_i^o(T) - \bar{H}_i^o(T_o)] + \sum_{i=1}^c n_i \bar{H}_i^o(T_o) + 68317 - n_g \bar{R}T + E^* \quad (A-2)$$

$$E^* = \int_{V_o}^V \left\{ T \left[ \frac{\partial p(T, \xi, \underline{n})}{\partial T} \right] - p(T, \xi, \underline{n}) \right\} d\xi \quad (A-3)$$

$$A = \sum_{i=1}^c n_i \bar{F}_i^o(T) + \bar{R}T \sum_{i=1}^c n_i \ln \left( \frac{n_i \bar{R}T}{p_o V} \right) - n_g \bar{R}T + A^* \quad (A-4)$$

$$A^* = - \int_{V_o}^V p(T, \xi, \underline{n}) d\xi \quad (A-5)$$

$$S = \frac{E - A}{T} \quad (A-6)$$

$$n_i = y_1^{r_{11}} y_2^{r_{21}} y_3^{-r_{31}} K_{p_i}(T) n_g^{\sum_{j=1}^c v_{1j}} e^{-\frac{1}{\bar{R}T} \sum_{j=1}^c v_{1j} \mu_j^*} \quad 1 \leq i \leq 20 \quad (A-7)$$

$$\mu_j^* = \left( \frac{\partial A^*}{\partial n_j} \right)_{T, V, n_k} = - \left[ \frac{\partial}{\partial n_j} \int_{V^0}^V p(T, \xi) d\xi \right]_{T, V, n_k} \quad (A-8)$$

$$y_1 + \sum_{i=1}^{20} r_{1i} n_i = 2 \quad (A-9)$$

$$y_2 + \sum_{i=1}^{20} r_{2i} n_i = 1 \quad (A-10)$$

$$y_3 - \sum_{i=1}^{20} r_{3i} n_i = 0 \quad (A-11)$$

The following definitions apply to the equations of this summary:

$$T_0 = 298.16^\circ K$$

$$p^0 = 1 \text{ atm}$$

$$V^0 = n_g \tilde{RT}/p^0 = \text{volume of } n_g \text{ mols (M}_0 \text{ gm) of mixture in the standard state}$$

$$\tilde{H}_1^0(T) = \text{molar enthalpy of the } i^{\text{th}} \text{ species in the standard state at temperature } T \text{ relative to the enthalpy of the reference materials } H_2, O_2, \text{ and e in the standard state at temperature } T_0$$

$$\tilde{H}_1^0(T_0) = \text{enthalpy of formation of one mol of the } i^{\text{th}} \text{ species in its standard state from the reference materials } (O_2, H_2, e) \text{ in their standard states at temperature } T_0$$

$$\tilde{F}_1^0(T) = \text{molar Gibbs free energy of the } i^{\text{th}} \text{ species in its standard state at temperature } T$$

$$\ln K_{p_1}(T) = - \sum_{j=1}^c \frac{v_{ij} \tilde{F}_j^0(T)}{\tilde{RT}}$$

$$v_{ij} = \text{stoichiometric coefficient of the } j^{\text{th}} \text{ component appearing in the } i^{\text{th}} \text{ reaction}$$

$y_1 = n_{21}$  = mols of atomic hydrogen in  $M_0$  gm of mixture

$y_2 = n_{22}$  = mols of atomic oxygen in  $M_0$  gm of mixture

$y_3 = n_{23}$  = mols of electrons in  $M_0$  gm of mixture

The standard state data for fifteen temperatures from 5000°K to 1,000,000°K (Region I) are tabulated in Ref. 11. Most of these data can also be found in Ref. 12. The standard state data in this region are given at the following temperatures (in degrees Kelvin): 5000, 7000, 10,000, 15,000, 20,000, 30,000, 50,000, 70,000, 100,000, 150,000, 200,000, 300,000, 500,000, 700,000, 1,000,000.

These data have been used for all diatomic species and for  $H_2O$ . However, all standard state data for the monatomic species above 5000°K have been obtained from a partition-function program developed by F. Gilmore at Rand. These (unpublished) results have been incorporated because they represent more recent data, and yield a significantly closer matching with the standard-state data of Ref. 24, which is used for the lower temperatures.

Standard state data for Region II are taken from the JANAF thermochemical tables.<sup>(24)</sup> The data are given for temperatures from 0 to 6000°K in 100-degree increments, plus data at 298°K.

Stoichiometric coefficients  $v_{ij}$  and  $r_{ak}$  appear in Tables 2 and 3, respectively.

## Appendix E

### SUMMARY OF THERMODYNAMIC RELATIONS BASED ON THE MODIFIED BKW EQUATION WITH $\beta = \beta(T)$ , $\kappa = \kappa(T)$

The working equations for Regions I and II, based on the modified BKW equation with variable parameters,  $\beta = \beta(T)$ ,  $\kappa = \kappa(T)$ , are presented here. These results were obtained by placing into the equations of Appendix A the thermal equation of state  $[p = p(T, V, n)]$  shown below, and carrying out the differentiation and integrations wherever it was possible to do so. The equations are:

$$p = \frac{n_g \tilde{R}T}{V} \left[ 1 + \kappa e^{\beta(T)x} \right] \quad (B-1)$$

$$x = \frac{k}{V(T + \theta)^\alpha} \quad (B-2)$$

$$k = \kappa(T) \sum_{i=1}^{23} k_i n_i \quad (B-3)$$

$$n_g = \sum_{i=1}^{23} n_i \quad (B-4)$$

$$E = \sum_{i=1}^{23} n_i [\tilde{H}_i^0(T) - \tilde{H}_i^0(T_0)] + \sum_{i=1}^{23} n_i \tilde{H}_i^0(T_0) \quad (B-5)$$

$$+ 68317 - n_g \tilde{R}T + n_g \tilde{R}T^2 \left\{ \left[ \frac{\alpha}{T + \theta} - \frac{\kappa'(T)}{\kappa(T)} - \frac{\beta'(T)}{\beta(T)} \right] \kappa e^{\beta(T)x} - \frac{\beta'(T)}{\beta^2(T)} \left[ 1 - e^{\beta(T)x} \right] \right\}$$

The enthalpy of formation of electrons,  $\bar{H}_{23}^0(T_0)$ , is zero, and their molar enthalpy difference is given by the relation

$$\bar{H}_{23}^0(T) - \bar{H}_{23}^0(T_0) = \frac{5}{2} \bar{R}(T - T_0)$$

$$n_j = K_j y_1^{r_{1j}} y_2^{r_{2j}} y_3^{-r_{3j}}, \quad 1 \leq j \leq 20 \quad (B-6)$$

$$K_j = K_{P_j}(T) \left( \frac{P^0}{RT} \right)^{\sum_{i=1}^{23} v_{ij}} \exp - \left\{ \left( \sum_{i=1}^{23} v_{ij} \right) \frac{[e^{\beta(T)x} - 1]}{\beta(T)} \right. \quad (B-7)$$

$$\left. + \frac{\kappa(T)}{k} n_g x e^{\beta(T)x} \sum_{i=1}^{23} v_{ij} k_i \right\}$$

$$y_1 + \sum_{i=1}^{20} r_{1i} n_i = 2 \quad (B-8)$$

$$y_2 + \sum_{i=1}^{20} r_{2i} n_i = 1 \quad (B-9)$$

$$y_3 - \sum_{i=1}^{20} r_{3i} n_i = 0 \quad (B-10)$$

$$v = V/M_0 \quad (B-11)$$

$$e = E/M_0 \quad (B-12)$$

See Appendix A for definitions of the symbols used in this summary of equations. Values for the stoichiometric coefficient  $v_{ij}$  and  $r_{oi}$  can be found in Tables 2 and 3. Table 3 also includes the sum

$$\sum_{j=1}^{23} v_{ij}$$

The covolume factors  $k_i$  and the sums

$$\sum_{j=1}^{23} v_{ji} k_j$$

appear in Table 4. Sources for the necessary standard state data are given in Appendix A.

# Appendix C

## SUMMARY OF THERMODYNAMIC RELATIONS BASED ON THE MODIFIED BKW EQUATION WITH $\beta = \beta(T)$ , $\kappa = \kappa(\bar{x})$

The working equations for Regions I and II, based on the modified BKW equation with variable parameters  $\beta = \beta(T)$ ,  $\kappa = \kappa(\bar{x})$ , are presented here. These results were obtained by placing into the equations of Appendix A the thermal equation of state  $[p = p(T, V, n)]$  shown below, and carrying out the differentiations and integrations wherever it was possible to do so. The equations are:

$$p = \frac{n \tilde{R} T}{V} [1 + x e^{\beta(T)x}] \quad (C-1)$$

$$x = \bar{x} \kappa(\bar{x}) \quad (C-2)$$

$$\bar{x} = \frac{\bar{k}}{V(T + \theta)^\alpha} \quad (C-3)$$

$$\bar{k} = \sum_{i=1}^{23} k_i n_i \quad (C-4)$$

$$n_g = \sum_{i=1}^{23} n_i \quad (C-5)$$

$$E = \sum_{i=1}^{23} n_i [\bar{H}_i^o(T) - \bar{H}_i^o(T_o)] + \sum_{i=1}^{23} n_i \bar{H}_i^o(T_o) + 68317 - n_g \tilde{R} T + \frac{\alpha n \tilde{R} T^2}{T + \theta} x e^{\beta(T)x} \quad (C-6)$$

$$- n_g \tilde{R} T^2 \beta'(T) \int_0^{\bar{x}} \xi \kappa^2(\xi) e^{\beta(T)\xi \kappa(\xi)} d\xi$$

The enthalpy of formation of electrons,  $\tilde{H}_{23}^0(T_0)$ , is zero, and their molar enthalpy difference is given by the relation

$$\tilde{H}_{23}^0(T) - \tilde{H}_{23}^0(T_0) = \frac{5}{2} \tilde{R}(T - T_0)$$

$$n_j = K_j y_1^{r_{1j}} y_2^{r_{2j}} y_3^{-r_{3j}}, \quad 1 \leq j \leq 20 \quad (C-7)$$

$$K_j = K_{P_j}(T) \left( \frac{P_0 V}{RT} \right)^{\sum_{i=1}^{23} v_{ij}} \exp - \left[ \left( \sum_{i=1}^{23} v_{ij} \right) \int_0^{\tilde{x}} \kappa(\xi) e^{\beta(T)\xi} \kappa(\xi) d\xi \right. \quad (C-8)$$

$$\left. + \frac{n}{k} \left( \sum_{i=1}^{23} v_{ij} k_i \right) x e^{\beta(T)x} \right]$$

$$y_1 + \sum_{i=1}^{20} r_{1i} n_i = 2 \quad (C-9)$$

$$y_2 + \sum_{i=1}^{20} r_{2i} n_i = 1 \quad (C-10)$$

$$y_3 - \sum_{i=1}^{20} r_{3i} n_i = 0 \quad (C-11)$$

$$v = V/M_0 \quad (C-12)$$

$$e = E/M_0 \quad (C-13)$$

See Appendix A for definitions of the symbols used in this summary of equations. Values for the stoichiometric coefficients  $v_{ij}$  and  $r_{\alpha i}$  can be found in Tables 2 and 3. Table 3 also includes the sum

$$\sum_{j=1}^{23} v_{ij}$$

The covolume factors  $k_i$  and the sums

$$\sum_{j=1}^{23} v_{ji} k_i$$

appear in Table 4. Sources for the necessary standard state data are given in Appendix A.

# Appendix D

## BRIEF OUTLINE OF THE COMPUTATIONAL METHOD FOR EQUILIBRIUM CALCULATIONS IN REGIONS I AND II

The Newton-Raphson iteration method is applied to the set of five simultaneous nonlinear equations in the five variables,  $y_1, y_2, y_3, y_4, y_5$ . The equations are solved for these variables as functions of volume and temperature. For the Hugoniot calculations, a sixth relation is added to the set of equations and the volume  $y_6$  is added to the list of variables.

The five equations are  $f_i = 0, i = 1 \dots 5$ , where the  $f_i$  are defined by the following relations

$$f_1 = y_1 + \sum_{i=1}^{20} r_{1i} n_i - 2$$

$$f_2 = y_2 + \sum_{i=1}^{20} r_{2i} n_i - 1$$

$$f_3 = y_3 - \sum_{i=1}^{20} r_{3i} n_i$$

$$f_4 = y_4 - y_1 - y_2 - y_3 - \sum_{i=1}^{20} n_i$$

$$f_5 = y_5 - \kappa(T) \sum_{i=1}^{23} k_i n_i$$

The Hugoniot relation is  $f_6 = 0$ , where

$$f_6 = \frac{E}{y_4 RT(1 + x e^x)} - \frac{v_o - y_6}{2y_6}$$

Appendices A, B, and C contain definitions of symbols used in these equations. In addition, the variables  $y_4$ ,  $y_5$ , and  $y_6$  have the following definitions.

$$y_4 = n_g = \text{total mols of mixture}$$

$$y_5 = k = \kappa(T) \text{ [average covolume factor of mixture]}$$

$$y_6 = v = \text{specific volume}$$

Linear estimates of the above equations, which are used in the iterative process, can be represented in the following form:

$$f_i(y_j^k) + \sum_j \left( \frac{\partial f_i}{\partial y_j} \right)^k dy_j^k = 0$$

where

$$y_j^{k+1} = y_j^k + dy_j^k$$

$i, j=1, \dots, 5$  for non-Hugoniot calculations

$i, j=1, \dots, 6$  for Hugoniot calculations

In these relations, the superscript  $k$  denotes the  $k^{\text{th}}$  iterate. For calculations on the Hugoniot, the initial guesses,  $y_j^1$ , were taken as the values given in Ref. 12. Initial guesses for  $y_j$  along an isotherm were taken from results of calculation of neighboring volume and temperature points.

Pressure and energy results can be obtained directly after the determination of the variables  $y_j$ ,  $j=1, \dots, 5$  or  $6$ , at a given  $T$  and  $v$  or  $T$ , respectively.

The accuracy criterion for convergence of the iterative process is

$$\max_j \left( \frac{|y_j^{k+1} - y_j^k|}{y_j^k} \right) \leq 10^{-5}$$

where  $\max$  signifies the maximum value overall  $j$ , at a given iteration ( $k$ ). This criterion also gives the result

$$\sum_i f_i^2 < 10^{-8}$$

This program is written in the MAP language and run on the IBM 7040/44 system.

REFERENCES

1. Papetti, R. A., and M. Fujisaki, *Thermochemical Relations for Water at High Temperatures and Pressures*, The Rand Corporation, RM-4970-PR, December 1966.
2. Latter, A., and R. Latter, *Equation of State of Water*, The Rand Corporation, RM-1492-AEC, May 1955.
3. Al'tschuler, L. V., A. A. Bakanova, and R. F. Trunin, Phase Transformations of Water Compressed by Strong Shock Waves, *Soviet Physics, Doklady*, Vol. 3, No. 4, January 1958, pp. 761-763.
4. Rice, M. H., and J. M. Walsh, Equation of State of Water to 250 Kilobars, *J. Chem. Phys.*, Vol. 26, No. 4, April 1957, pp. 824-830.
5. Feynman, R. P., N. Metropolis, and E. Teller, Equations of State of Elements Based on the Generalized Fermi-Thomas Theory, *Phys. Rev.*, Vol. 75, No. 10, May 1949, pp. 1561-1572.
6. Knopoff, L., Equation of State for Water at High Pressure, *J. Chem. Phys.*, Vol. 28, No. 6, June 1958, pp. 1067-1069.
7. Walker, W. A., and H. M. Sternberg, The Chapman-Jouguet Isentrope and the Underwater Shockwave Performance of Pentolite, in *The Fourth Symposium on Detonation*, October 12-15, 1965, Preprints, Vol. 1, U.S. Naval Ordnance Laboratory, White Oak, Silver Spring, Maryland, pp. 156-169.
8. Howard, J. C., *Thermodynamic Data for Water*, University of California Radiation Laboratory, UCRL-6455-T, April 1961.
9. Snay, H. G., and I. Stegun, *Auxiliary Functions for Thermodynamic Calculations Based on the Kistiakowsky-Wilson Equation of State (Kirkwood-Montroll I - Functions)*, U.S. Naval Ordnance Laboratory, NAVORD 1732, January 1951.
10. Rosenbaum, J. H., *An Equation of State for Water at Extreme Pressures*, U.S. Naval Ordnance Laboratory, NAVORD 3847, November 1954.
11. Snay, H. G., and J. F. Butler, *Equation of State for Water*, U.S. Naval Ordnance Laboratory, NAVORD 4181, November 1956.
12. Gleysal, A. N., and H. G. Snay, *Equation of State of Water*, U.S. Naval Ordnance Laboratory, NAVORD 6749, December 1959.
13. Mader, C. L., *Detonation Performance Calculations Using the Kistiakowsky-Wilson Equation of State*, Los Alamos Scientific Laboratory, LA 2613, October 1961.

14. Mader, C. L., *Detonation Properties of Condensed Explosives Computed Using the Becker-Kistiakowsky-Wilson Equation of State*, Los Alamos Scientific Laboratory, LA 2900, February 1963.
15. Cowan, R. D., and W. Fickett, Calculation of the Detonation Properties of Solid Explosives with the Kistiakowsky-Wilson Equation of State, *J. Chem. Phys.*, Vol. 24, No. 5, May 1956, pp. 932-939.
16. Christian, E. A., and H. G. Snay, *Analysis of Experimental Data on Detonation Velocities*, U.S. Naval Ordnance Laboratory, NAVORD 1508, February 1951.
17. Courant, R., and K. O. Friedrichs, *Supersonic Flow and Shock Waves*, Interscience Publishers, Inc., New York, 1948.
18. Fickett, W., *Intermolecular Potential Functions for Some Simple Molecules From Available Experimental Data*, Los Alamos Scientific Laboratory, LA 2665, July 1962.
19. Fickett, W., Calculation of the Detonation Properties of Condensed Explosives, *Physics of Fluids*, Vol. 6, No. 7, July 1963, pp. 997-1006.
20. Fickett, W., W. W. Wood, and Z. W. Salsburg, Investigations of the Detonation Properties of Condensed Explosives with Equations of State Based on Intermolecular Potentials. I. RDX With Fixed Product Composition, *J. Chem. Phys.*, Vol. 27, No. 6, December 1957, pp. 1324-1329.
21. Fickett, W., *Detonation Properties of Condensed Explosives Calculated with an Equation of State Based on Intermolecular Potentials*, Los Alamos Scientific Laboratory, LA 2712, May 1962.
22. Keeler, R. N., B. J. Alder, and M. van Thiel, *Corresponding States at Small Interatomic Distances*, University of California Radiation Laboratory, UCRL-7907 Rev. I, November 1964.
23. Hirschfelder, J. O., C. F. Curtiss, and R. B. Bird, *Molecular Theory of Gases and Liquids*, Wiley, New York, 1954.
24. Joint Army-Navy-Air Force Thermochemical Panel, *JANAF Interim Thermochemical Tables*, ( $H_2O$ ), prepared by the Thermal Laboratory of the Dow Chemical Company, March 1961.
25. Papetti, R. A., and M. Fujisaki, The Rice and Walsh Equation of State for Water: Discussion, Limitations, and Extension, *J. Appl. Phys.*, Vol. 39, No. 12, November 1968, pp. 5412-5421.